Unclassified

SECURITY CLASSIFICATION OF THIS PAGE

(2)

REPORT DOCUMENTATION PAGE

1a. REPORT SECURITY CLASSIFICATION UNCLASSIFIED	1b. RESTRICTIVE MARKINGS DTIC FILE COPY
2a. SECURITY CLASSIFICATION AUTHORITY AD-A204 555	3. DISTRIBUTION/AVAILABILITY OF REPORT Approved for public release, distribution unlimited
	5. MONITORING ORGANIZATION REPORT NUMBER(S) AFOSR-TR- 89-0099
6a. NAME OF PERFORMING ORGANIZATION Northwestern University	6b. OFFICE SYMBOL (If applicable)
6c. ADDRESS (City, State and ZIP Code) Department of Civil Engineering The Technological Institute Evanston, IL 60208	7a. NAME OF MONITORING ORGANIZATION USAF, AFSC Air Force Office of Scientific Research 7b. ADDRESS (City, State and ZIP Code) Building 410 Bolling AFB, D.C. 20332-6448
8a. NAME OF FUNDING/SPONSORING ORGANIZATION	8b. OFFICE SYMBOL (If applicable) NA
8c. ADDRESS (City, State and ZIP Code) same as 7b.	9. PROCUREMENT INSTRUMENT IDENTIFICATION NUMBER F49620-88-C-0011 10. SOURCE OF FUNDING NOS.

PROGRAM ELEMENT NO.	PROJECT NO.	TASK NO.	WORK UNIT NO.
FQ8671	2302	[redacted] B1	[redacted]

11. TITLE (Include Security Classification) FISSION-FUSION ADAPTIVITY IN FINITE ELEMENTS FOR NONLINEAR DYNAMICS OF SHELLS (U)

12. PERSONAL AUTHOR(S)
T. Belytschko

13a. TYPE OF REPORT	13b. TIME COVERED	14. DATE OF REPORT (Yr., Mo., Day)	15. PAGE COUNT
Annual Technical	FROM 10/01/87 TO 09/30/88	30 November 1988	65

16. SUPPLEMENTARY NOTATION

DTIC ELECTE S 21 FEB 1989 D

17 COSATI CODES			18. SUBJECT TERMS (Continue on reverse if necessary and identify by block number)
FIELD	GROUP	SUB. GR.	
			finite elements, adaptive meshes, shells

19. ABSTRACT (Continue on reverse if necessary and identify by block number)

An adaptive finite element procedure is developed for the transient analysis of nonlinear shells. The scheme is an h-method which employs fission and fusion of elements to adaptively refine and coarsen the mesh. Incremental work and deviation of the bilinear finite element approximation to the shell from a Kirchhoff-Love surface are used as error criteria for adaptivity. The example problems show that the adaptive schemes are capable of achieving substantial improvements in accuracy for a given computational effort. They include both material and geometric nonlinearities and local and global buckling.

20. DISTRIBUTION/AVAILABILITY OF ABSTRACT	21. ABSTRACT SECURITY CLASSIFICATION
UNCLASSIFIED/UNLIMITED ☑ SAME AS RPT. ☑ DTIC USERS ☑	UNCLASSIFIED

22a. NAME OF RESPONSIBLE INDIVIDUAL	22b. TELEPHONE NUMBER (Include Area Code)	22c. OFFICE SYMBOL
[redacted] Dr. Anthony Amos	(202) 767-4937	NA

DD FORM 1473, 83 APR EDITION OF 1 JAN 73 IS OBSOLETE.

Unclassified

SECURITY CLASSIFICATION OF THIS PAGE

FISSION-FUSION ADAPTIVITY IN FINITE ELEMENTS FOR NONLINEAR DYNAMICS OF SHELLS

Principal Investigator: Ted Belytschko

Annual Technical Report

October 1, 1987 - September 30, 1988

Department of Civil Engineering
Northwestern University
Evanston, Illinois 60208

Air Force Research Grant F49620-88-C-0011

TABLE OF CONTENTS

	Page
PREFACE	iii
1. INTRODUCTION	1
2. FINITE ELEMENT FORMULATION	5
3. FISSION AND FUSION ADAPTIVITY	12
Fission-Fusion Criteria	15
Fission Process	16
Fusion Process	18
4. DATA STRUCTURE	19
5. NUMERICAL EXAMPLES	25
6. CONCLUSIONS	30
REFERENCES	32
Table 1	34
LIST OF FIGURES	35
Figures 1-23	37-62

PREFACE

This research was conducted under the direction of Professor Ted Belytschko. The following research personnel participated in the research program: Dr. Bak Leong Wong and Mr. Edward J. Plaskacz.

The following papers, which were supported by AFOSR under this grant or under grant F49620-85-C-0128 during the preceding years of support, were published in this time period:

N. Carpenter, H. Stolarski, and T. Belytschko, "Improvements in 3-Node Triangular Shell Elements," International Journal for Numerical Methods in Engineering, 23(9), 1643-1667, 1986.

H. Stolarski and T. Belytschko, "On the Equivalence of Mode Decomposition and Mixed Finite Elements Based on the Hellinger-Reissner Principle. Part I: Theory," Computer Methods in Applied Mechanics and Engineering, 58(3), 249-265, 1986.

H. Stolarski and T. Belytschko, "On the Equivalence of Mode Decomposition and Mixed Finite Elements Based on the Hellinger-Reissner Principle. Part II: Applications," Computer Methods in Applied Mechanics and Engineering, 58(3), 265-285, 1986.

H. Stolarski and T. Belytschko, "Limitation Principles for Mixed Finite Elements Based on the Hu-Washizu Variational Formulation," Computer Methods in Applied Mechanics and Engineering, 60(2), 195-216, 1987.

T. Belytschko, W. K. Liu and J. S.-J. Ong, "Mixed Variational Principles and Stabilization of Spurious Modes in the 9-Node Element," Computer Methods in Applied Mechanics and Engineering, 62(3), 275-292, 1987.

B. L. Wong and T. Belytschko, "Assumed Strain Stabilization Procedure for the 9-Node Lagrange Plane and Plate Elements," Engineering Computations, 4(3), 229-239, 1987.

W. K. Liu, H. Chang, J.-S. Chen, and T. Belytschko, "Arbitrary Lagrangian-Eulerian Petrov-Galerkin Finite Elements for Nonlinear Continua," Computer Methods in Applied Mechanics and Engineering, 68(3), 259-310, 1988.

The following doctorate was supported by this research:

Bak Leong Wong, "Shell Finite Elements: A New Resultant Stress Formulation and Stabilization," December 1987.

1. INTRODUCTION

The nonlinear transient analysis of structures is a particularly promising field for adaptive procedures, because, among the various classes of structural finite element applications, it is computationally the most demanding. It is not uncommon for simulations of crashes of automobiles or aircraft to require 10 to 20 hours of CRAY time. Furthermore, in this class of applications, a priori selection of an appropriately refined mesh is most difficult, since the areas of the mesh which need to be refined depend on the evolution of the response, which cannot be foreseen by the analyst. Thus, while expert systems may prove to be quite effective in helping a user design appropriate meshes for linear-elastic, static problems, it is not possible in a typical nonlinear transient problem, such as the simulation of a high-energy deposition on a missile nose or a front-end crash of an automobile. In this type of analysis, the computational power must be focused on those parts of the mesh which undergo the most severe deformation, such as hinging and wrinkling, and the sites of such deformations are not determinable a priori. Furthermore, it is desirable to start various types of simulations, such as a frontal and side crash, with the same mesh and let the response dictate any refinement.

While nonlinear transient analysis is one of the most promising areas for adaptive procedures, it is also the most challenging. Perusal of reviews of the field of adaptive finite elements recently written by Noor and Babuska (1987) and Oden and Demkowicz (1988) reveals that the bulk of the theoretical work has been devoted to determining local error estimates for linear static problems; these estimates are used to select the elements or subdomains to be refined. These error estimates have evolved into two main types:

1. residual error criteria based on the magnitude of the residual in the governing equations;
2. error indicators based on interpolation methods.

A difficulty in applying these methods to shells is that in the most effective elements for shell analysis, namely bilinear quadrilateral elements such as described in Belytschko, Lin, and Tsay (1984) and in Hallquist and Benson (1986), even the shape of the shell is not adequately represented. In other words, while the momentum residual in the equations of motion for the bilinear description of the shell may be small, the errors may be quite large due to discrepancies between the configuration of the shell surface and the bilinear finite element representation.

However, this drawback provides an opportunity, for in fact it is in the regions of maximal deviation between the bilinear representation and the shell surface that the finite element mesh is most inadequate. Since an average normal to the shell surface can be estimated at all times, the deviation of the bilinear representation from a more accurate approximation to the shell surface can be computed and used to indicate where mesh refinement will prove useful. In fact, the deviation of a bilinear element from a smooth shell midsurface can be related to the angle between adjacent elements.

The regions where the largest angles occur between adjacent elements are not the only regions which require refinement. Three other sources of important errors in shells treated by bilinear shell elements with hourglass control are regions where:

1. high gradients of membrane stresses occur;
2. significant amounts of energy are dissipated in the hourglass modes;

3. high uniform compressive strains lead to the possibility of buckling.

Adaptive methods can be used to achieve two distinct but related goals:

1. to achieve a given level of accuracy without regard to computer resources;
2. to achieve the best solution with a specified amount of computer resources.

We have chosen the second goal. This choice is based on two reasons:

1. It is impossible at this time, with the available mathematical tools for error estimation, to estimate the local error in a nonlinear transient solution.
2. In most computer systems, the fast memory allocated to a run must be set at the beginning of the run.

Therefore, the philosophy of the adaptive process described here is to obtain the most accuracy for a given set of computational resources. As will be seen in the examples, this philosophy is quite effective. By using an adaptive mesh, it is generally possible to obtain a solution of comparable accuracy with far fewer elements, and hence, less computational resources than with a fixed mesh.

The effort described here is focused on adaptivity in the context of the nonlinear transient analysis of shells with explicit time integration. This is the most commonly used method for problems characterized by severe, dynamic deformations. In addition, we carefully consider the demands of vectorization, since most current supercomputers use this technique for accelerating computations. From the viewpoint of the programmer, vectorization is like a SIMD (single instruction, multiple data stream) computer. Blocks of elements must be arranged so that they all do the same operation; consequently, recursive calculations and conditional statements

are quite detrimental. One of the major competitors of the next generation of supercomputers, the CONNECTION machine, is also a SIMD computer, so these limitations may be with us for a long time. This has many ramifications in the choice of adaptivity and its implementation.

The paper is organized as follows. Section 2 describes the basic method used for the nonlinear transient analysis of shells. Section 3 describes the type of adaptivity used, the reasons for the choice, and its implementation. Section 4 describes the data structure. Section 5 describes some results obtained with this method, with the emphasis on comparisons with nonadaptive meshes. Conclusions and further discussions are given in Section 6.

2. FINITE ELEMENT FORMULATION

The shape of the midsurface is described in this finite element model by

$$x_i = N_I(\xi)\, x_{iI} \tag{2.1}$$

where x_{iI} are the coordinates of node I and $N_I(\xi)$ are the bilinear isoparametric shape functions. Lowercase subscripts designate Cartesian components, and uppercase subscripts designate node numbers; repeated indices are summed over their range, 4 for uppercase, 3 for lowercase.

The shape functions $N_I(\xi)$ are functions of the reference variables ξ_i, $i = 1,2$, also written as $\xi_1 = \xi$, $\xi_2 = \eta$, and they are given by

$$N_I = \frac{1}{4}\,(1 + \xi_I\xi)\,(1 + \eta_I\eta) \tag{2.2}$$

where ξ_I and η_I are the coordinates of the nodes at the corners of the reference domain defined by $-1 \le \xi \le 1$, $-1 \le \eta \le 1$. Note that unless a mesh of these elements is quite refined, they provide a rather poor model for the curved surface of a shell. In a regular mesh on a cylindrical shell, these elements are in fact all flat, and any interaction between flexure and membrane response only occurs at the nodes. Furthermore, in a region of large curvature, this model can deteriorate even more severely with very large angles between adjacent elements. However, before discussing this further, the basic mechanics of this finite element formulation will be described.

In the formulation, two types of coordinates are used in addition to the global Cartesian coordinates:

1. for each element, an element coordinate system $(\hat{x},\hat{y},\hat{z})$ with base vectors $\underset{\sim}{e}_1$, $\underset{\sim}{e}_2$, and $\underset{\sim}{e}_3$ is defined so that $\underset{\sim}{e}_1$ and $\underset{\sim}{e}_2$ are tangent to the midsurface and rotate with the element;
2. for each node, a triad $\underset{\sim}{b}_i$ is defined so that it rotates with the node, with $\underset{\sim}{b}_3$ normal to the midsurface of the shell in the undeformed configuration.

Whereas in the original formulation of Belytschko, Lin, and Tsay (1984) the original orientation of $\underset{\sim}{b}_i$ was arbitrary, it is used here to locate new nodes created in the adaptive process and therefore must initially be approximately normal to the midsurface of the shell.

The deformation of the element is governed by the Mindlin-Reissner hypothesis, which allows transverse shear but requires the normal to remain straight, so the velocity of a generic point in the shell is given in terms of the velocity of the midsurface v_i^m and the angular velocity ω_i by

$$v_i = v_i^m - \hat{z}\,(\underset{\sim}{e}_3 \times \underset{\sim}{\omega})_i \tag{2.3}$$

where $\hat{z}$, by the definition of the element coordinates, is the distance of a point from the midsurface.

The velocity field is given by

$$v_i^m = N_I \, v_{iI}^m \tag{2.4}$$

$$\omega_i = N_I \, \omega_{iI} \tag{2.5}$$

The strain rates (velocity strains or stretching) are given in terms of the nodal velocities in the element coordinate system by

$$\hat{d}_{xx} = \frac{\partial \hat{v}_x^m}{\partial \hat{x}} + \hat{z} \frac{\partial \hat{\omega}_y}{\partial \hat{x}} \tag{2.6a}$$

$$\hat{d}_{yy} = \frac{\partial \hat{v}_y^m}{\partial \hat{y}} - \hat{z} \frac{\partial \hat{\omega}_x}{\partial \hat{y}} \tag{2.6b}$$

$$2\hat{d}_{xy} = \frac{\partial \hat{v}_x^m}{\partial \hat{y}} + \frac{\partial \hat{v}_y^m}{\partial \hat{x}} + \hat{z} \left(\frac{\partial \hat{\theta}_y}{\partial \hat{y}} - \frac{\partial \hat{\theta}_x}{\partial \hat{x}} \right) \tag{2.6c}$$

$$2\hat{d}_{xz} = \frac{\partial \hat{v}_z^m}{\partial \hat{x}} + \hat{\theta}_y \tag{2.6d}$$

$$2\hat{d}_{yz} = \frac{\partial \hat{v}_z^m}{\partial \hat{y}} - \hat{\theta}_x \tag{2.6e}$$

Since the element uses one-point quadrature, the strains are evaluated at a single point, the origin of the reference plane which is given by $\xi = \eta = 0$.

The velocity strains at this point are given by

$$\hat{d}_{xx} = B_{xI}\,\hat{v}_{xI} + \hat{z}\,(B'_{xI}\,\hat{v}_{xI} + B_{xI}\,\hat{\omega}_{yI}) \tag{2.7a}$$

$$\hat{d}_{yy} = B_{yI}\,\hat{v}_{yI} + \hat{z}\,(B'_{yI}\,\hat{v}_{yI} - B_{yI}\,\hat{\omega}_{xI}) \tag{2.7b}$$

$$\hat{d}_{xy} = B_{yI}\,\hat{v}_{xI} + B_{xI}\,\hat{v}_{yI} + \hat{z}\,(B'_{yI}\,\hat{v}_{xI} + B'_{xI}\,\hat{v}_{yI} - B_{xI}\,\hat{\omega}_{xI} + B_{yI}\,\hat{\omega}_{yI}) \tag{2.7c}$$

$$2\hat{d}_{xz} = B_{xI}\,\hat{v}_{zI} + s_I\,\hat{\omega}_{yI} \tag{2.7d}$$

$$2\hat{d}_{yz} = B_{yI}\,\hat{v}_{zI} - s_I\,\hat{\omega}_{xI} \tag{2.7e}$$

where

$$s_I = N_I(\underline{0}) = \frac{1}{4}[1,1,1,1] \tag{2.8a}$$

$$B_{xI} = \frac{\partial N_I(\underline{0})}{\partial \hat{x}} = \frac{1}{2A}[\hat{y}_{24}, \hat{y}_{31}, \hat{y}_{42}, \hat{y}_{13}] \tag{2.8b}$$

$$B_{yI} = \frac{\partial N_I(\underline{0})}{\partial \hat{y}} = \frac{1}{2A}[\hat{x}_{42}, \hat{x}_{13}, \hat{x}_{24}, \hat{x}_{31}] \tag{2.8c}$$

$$B'_{iI} = \frac{1}{2A}\begin{bmatrix} \hat{n}_{y,\eta} - C\,\hat{y}_{,\eta} & -(\hat{n}_{y,\xi} - C\,\hat{y}_{,\xi}) \\ -(\hat{n}_{x,\eta} - C\,\hat{x}_{,\eta}) & \hat{n}_{x,\xi} - C\,\hat{x}_{,\xi} \end{bmatrix} \begin{Bmatrix} N_{I,\xi} \\ N_{I,\eta} \end{Bmatrix} \tag{2.8d}$$

$$C = \frac{1}{2A}(\hat{x}_{,\xi}\,\hat{n}_{y,\eta} + \hat{y}_{,\eta}\,\hat{n}_{x,\xi} - \hat{x}_{,\eta}\,\hat{n}_{y,\xi} - \hat{y}_{,\xi}\,\hat{n}_{x,\eta}) \tag{2.8e}$$

$$x_{IJ} = x_I - x_J \tag{2.8f}$$

$$y_{IJ} = y_I - y_J \tag{2.8g}$$

and $\underset{\sim}{n}$ is the normal to the shell.

The nodal forces are computed from the stresses by one-point quadrature, which yields

$$\hat{f}_{xI} = A\,(B_{xI}\,\sigma_{xx} + B'_{xI}\,m_{xx} + B_{yI}\,\sigma_{xy} + B'_{yI}\,m_{xy}) \tag{2.9a}$$

$$\hat{f}_{yI} = A\,(B_{yI}\,\sigma_{yy} + B'_{yI}\,m_{yy} + B_{xI}\,\sigma_{xy} + B'_{xI}\,m_{xy}) \tag{2.9b}$$

$$\hat{f}_{zI} = A\,(B_{yI}\,\sigma_{yz} + B_{xI}\,\sigma_{xz}) \tag{2.9c}$$

$$\hat{m}_{xI} = -A\,(B_{yI}\,m_{yy} + B_{xI}\,m_{xy} + s_I\,\sigma_{yz}) \tag{2.9d}$$

$$\hat{m}_{yI} = A\,(B_{xI}\,m_{xx} + B_{yI}\,m_{xy} + s_I\,\sigma_{xz}) \tag{2.9e}$$

where

$$\sigma_{ij} = \int_{-h/2}^{h/2} \hat{\sigma}_{ij}\,\hat{dz} \tag{2.9f}$$

$$m_{ij} = \int_{-h/2}^{h/2} \hat{\sigma}_{ij} \hat{z} \, d\hat{z} \tag{2.9g}$$

and h is the thickness.

The one-point quadrature element is rank-deficient, so it is associated with spurious singular modes, as described in Belytschko, Lin, and Tsay (1984). Their control is also described therein.

The incremental work is computed in each element by

$$\Delta W_e^{int} = \int \Delta t \, (\underline{d}^{n+\frac{1}{2}})^T \, (\underline{\sigma}^n + \underline{\sigma}^{n+1}) \, dV \tag{2.10a}$$

where

$$\underline{d}^T = [d_{xx}, \, d_{yy}, \, d_{xy}, \, d_{xz}, \, d_{yz}] \tag{2.10b}$$

$$\underline{\sigma}^T = [\sigma_{xx}, \, \sigma_{yy}, \, \sigma_{xy}, \, \sigma_{xz}, \, \sigma_{yz}] \tag{2.10c}$$

and Δt is the time increment; superscripts indicate the time step. This quantity is used to check stability and as a criterion for mesh adaptation in some of the studies.

3. FISSION AND FUSION ADAPTIVITY

The type of adaptivity which has been adopted here is an h-type, where the mesh is selectively refined in parts of the domain during the evolution of the solution. In addition, the refined elements are fused when they are no longer needed, so that computational power is not wasted on those parts of the domain which no longer undergo a changing deformation pattern. The motivation for including the fusion process is that in nonlinear transient problems, certain parts of the domain in effect "freeze", so that coarse meshes can capture their behavior effectively.

For the purpose of explaining the rationale for our use of h-type adaptivity, it is worthwhile to summarize other types of adaptivity.

Noor and Babuska (1987) describe the four forms of mesh enrichment as:

1. h-method: Grid intervals are either increased by combining elements or decreased by splitting elements into smaller quadrilaterals.
2. r-method: Node relocation.
3. p-method: Element trial functions are replaced by higher degree polynomials where more accuracy is needed.
4. h-p method: A simultaneous application of both the h- and p-methods.

Node relocation (r-method) has the following disadvantages in nonlinear shell problems:

1. In history-dependent materials, such as elastic-plastic materials, the migration of material particles between elements, which is a by-product of the r-method, is difficult to treat and always results in material history diffusion.

2. It is difficult to design algorithms which keep the nodes on a smooth surface.
3. The extra accuracy achievable by the r-method is quite limited, since the number of nodes and elements is fixed.

The advantage of the r-method over the other methods is that it does not require a special data structure. In fact, any transient finite element program already contains all data required for r-adaptivity. However, this advantage is outweighed by the disadvantages listed above.

The p-method has the following disadvantages:

1. It is difficult to compute an effective lumped mass matrix for higher order elements, but without a lumped mass, explicit time integration is quite inefficient.
2. The critical time step for explicit time integration decreases markedly as the order of the element increases for both consistent and lumped masses.
3. Higher order elements are associated with the appearance of an optical mode, and these add to the noise of a solution; see Belytschko and Mullen (1978).

The major disadvantage of the h-adaptive procedure is that it involves the creation and destruction of nodes and elements and therefore requires an elaborate data structure, since the interrelationships of old and new nodes and elements must also be known. However, this disadvantage is basically surmountable, whereas those of the other methods are not.

For these reasons, the h-method has been chosen as the mesh-enrichment strategy in our formulation. The aim of this method is to allocate elements to regions of the mesh where mesh refinement is necessary, in order to obtain the most accuracy for a given amount of computational resources. In the h-method mesh-enrichment strategy, a single quadrilateral element may be

refined or split into four equal-sized smaller elements, or four elements may be derefined or combined into a single element. We shall refer to the refinement of a single "parent" quadrilateral element into four smaller "sibling" quadrilateral elements as "fission" and to the derefinement of four siblings into their parent as "fusion". These processes are illustrated in Fig. 1.

For the purpose of organization, any group of four elements which is created by fission is called a "molecule". The original elements in a mesh are called "patriarchs" or generation-0, and they cannot be fused. The elements generated by adaptivity are called "descendants".

There are three aspects to the implementation of fission-fusion adaptivity:

1. criteria for fission and fusion (the evaluation of these criteria is called an assessment or a judgment);
2. the initial conditions for element and nodal variables at the nodes and elements which are created by fission;
3. the initial conditions for element and nodal variables at the nodes and elements which are created by fusion.

Five parameters have been established to control element allocation:

1. FACTOR = fraction of elements to be considered for fission.
2. NJUMP = frequency of mesh assessment in time steps.
3. NBEGA = time step of the initial fission-fusion assessment.
4. NCYCLE = number of consecutive assessments in which an element must be chosen for fission (fusion) before it can be fissioned (fused).
5. MAXGEN = maximum number of descendant generations.

Fission-Fusion Criteria

Two criteria have been adopted for making judgments on fission-fusion:

1. an incremental internal work criterion;
2. a discontinuity criterion based on the angle between two adjacent elements.

According to the incremental internal work criterion, the elements which are fissioned are those which sustain the largest increment in internal work. Because this variable usually has an oscillatory character in an explicit solution of a transient problem, the judgment is made on the basis of the total incremental work done over a specified number of time steps, ranging from 5 to 20. For the purpose of comparing elements of different sizes, the total incremental energy in a molecule is used as the criterion. Thus, fusion is indicated whenever the incremental work in a group of four elements which has been created by a previous fission is smaller than the incremental energy in other molecules.

Even with the filtering that is brought about by taking the incremental work over five steps, the incremental work criterion can lead to an oscillatory pattern of fission followed by fusion in many molecules in a transient process. Therefore, a time delay has been included which prevents fission or fusion unless it is indicated by two consecutive judgments. This type of retardation of the adaptive process appears to be needed in explicit treatments of nonlinear structural dynamics with adaptive meshes if excessive "churning" between fission and fusion is to be avoided.

The second criterion we have studied is based on the change in angle between two elements. The basis for this criterion is that one of the largest sources of errors is the inability of the piecewise bilinear elements to capture the correct shape and moment and curvature fields of the shell as the deformation localizes. Severe deformation in shells is usually

associated with large curvatures; since the bilinear element cannot represent large curvatures directly, it is associated with severe "kinking" between elements, which can be detected by monitoring the angle between elements. For those elements which satisfy the angle criterion for fission, both elements on each side of the line are subdivided into four elements.

An advantage of the angle criterion over the incremental work criterion is that it can be applied to more than one level of fission-fusion without need of additional parameters. The incremental work criterion, if it is to be used for two levels of fission-fusion, requires the specification of a ratio of incremental work in the refined elements to that in the coarse elements at which the second level of fission is initiated.

Since it is difficult to relate any of these criteria to the ultimate accuracy of a solution, one technique we have used is to simply specify the maximum number of elements and use the criteria to select where those elements are placed. In this procedure, we start with a uniform mesh which contains the maximum number of elements allowed. After five time steps, the elements are fissioned or fused according to the magnitudes of the amplitudes of their error indicators until the maximum number of elements is obtained.

Fission Process

When an element is fissioned next to an unfissioned element, as shown in Fig. 2, nodes are created adjacent to unsplit sides, so they cannot be handled by the usual equations of motion. In order to correctly handle compatibility, these nodes must be treated as "slave" nodes which are driven by the adjacent "master" nodes. In addition, in order to introduce a good representation of the shell as quickly as possible, it is useful to use the

nodal vectors $\underset{\sim}{b}_i$ for an approximation of the curved Kirchhoff-Love surface on which the new nodes are placed.

The procedure for setting the initial configuration of the nodes is as follows. The surface is approximated by

$$x_I = x_{iI} N_I + \sum_{J=1}^{4} S_{Ji} \tag{3.1}$$

where

$$S_{1i} = (\phi_{12} H_1(\xi) + \phi_{21} H_2(\xi)) n_i |\underset{\sim}{r}_{ij}| (N_1 + N_2) \tag{3.2}$$

where $H_I(\xi)$ are the Hermite interpolants, so that $H_{I,\xi}(\xi_J) = \delta_{IJ}$ and ϕ_{IJ} is the slope of the Kirchhoff-Love surface relative to the bilinear approximation, which is obtained by

$$\phi_{IJ} = -(\underset{\sim}{b}_3 \cdot \underset{\sim}{r}_{IJ})/|\underset{\sim}{r}_{IJ}| \tag{3.3}$$

The initial velocities of the nodes are obtained from the bilinear interpolation (2.1). The initial element variables for the elements are

taken from the parent element. The mass matrix is reassembled after fission. Nodes which are formed at sides which are continuous sides of the adjacent elements are considered slave nodes. All other new nodes are master nodes. Thus, an interior node is always a master node, but if only a single, isolated element undergoes fission, all other new nodes are slave nodes.

Fusion Process

In the fusion process, no new nodes are created; the velocities and displacements at the nodes which remain are assumed to be continuous during fusion. The number of elements is reduced from four to one; the historical state variables (stress components and yield) are taken to be the area-weighted average of the parent element stresses. State variables such as the yield stress cannot be adjusted so they remain completely consistent. For example, even if all of the elements in a molecule are plastic, because of the convexity of the yield function, the yield stress of the fused element will always be elastic (unless all four elements are along the same linear part of a yield surface). However, this does not present difficulties in an explicit computer program. Note that if all four elements are elastic, the convexity of the yield surface guarantees that the fused element is elastic; also, it is never possible for the state in a fused element to lie outside the yield surface.

4. DATA STRUCTURE

An important ingredient of a general-purpose h-adaptive program is the data structure. In designing a data structure, compromises must be made to conserve storage and avoid excessive computation time. We viewed these trade-offs from the perspective of implementation on a vectorized computer, where recursive operations must be avoided as much as possible. Therefore, we adopted the viewpoint that recursive calculations with a low fixed limit could be permitted during assessments but not during the routine time integration process. The upshot of this viewpoint is that the regular data structure is retained for the mesh, so element computations require no recursive computations; subsidiary information that allows retracing the mesh to its parent configuration may involve recursive calculations for its interpretation. The latter is important because in an h-adaptive algorithm, fission splits a single parent quadrilateral into four smaller sibling quadrilateral elements. In fusion, it is necessary to retrace this process in reverse. These relationships among elements can be expressed most compactly through a hierarchal or tree-type data structure. However, since fission-fusion only occurs every 10 to 100 time steps, this does not compromise vectorization much.

In describing data structures for h-adaptive procedures, it is best to begin with Rheinboldt and Mesztenyi (1980), who introduced a general labeled tree structure for two-dimensional finite element meshes which compactly describes the history and current state. Their algorithm emphasizes a minimization of storage and makes extensive use of recursive programming techniques. However, the traditional finite element data structure has been abandoned. The distinction between nodes and elements is blurred in their method since they deal with points. For example, an undivided quadrilateral

is designated by its centerpoint number. Upon refinement, the node created at the center of the parent quadrilateral is designated by this same centerpoint number. Thus, a number associated with a point may refer to either an element or a node at different stages of the adaptive process. Since emphasis is placed on the minimization of storage, extensive use of the tree structure is made to recalculate nodal coordinates, element interrelationships, and nodal interrelationships (master-slave). Thus, substantial effort is expended in tree travel, which is essentially a recursive process and does not lend itself to vectorization. Furthermore, as a consequence of the abandonment of the traditional finite element data structure, recursive calculations are needed even during routine element calculations, which we feel has detrimental effects on a vectorized computer.

Devloo, Oden, and Stroubelis (1987) present an augmented data structure, consisting of the traditional nodal coordinate and element connectivity arrays supplemented by a NELCON (neighboring element connectivity) array. Their data structure is constructed with the tacit assumption of the 1-irregular rule: neighboring elements can be at most one generation apart, or, in other words, each element borders on at most two other elements on any side. Thus, a NELCON array is an array with dimensions $8 \times$ NELE, where NELE is the number of elements. Refinement of an element in the data structure of Devloo, Oden, and Stroubelis (1987) results in a group consisting of four new elements. Their data structure also requires recursive calculations in the routine calculations.

The data structure described here differs from the preceding two in that the full finite element data structure is retained in conjunction with some additional data which is chosen so that no recursive calculations are necessary except during fusion. This data structure closely parallels the

traditional finite element data structure but is nonetheless a hierarchal data structure. The cornerstones of this data structure are the "forest of trees" concept employed by Ewing (1986) and the 1-irregular rule described by Bank and Sherman (1980); see also Bank, Sherman, and Weiser (1983). Since it retains the traditional finite element connectivity array, this data structure can be readily implemented into existing finite element codes.

The data commences with an initial coarse mesh of elements called generation-0 or patriarchs. This initial mesh must be adequate for describing the shape of the structure, loading, material properties, and boundary conditions. The patriarchs are never fused. A "family" is defined as a set of elements which are descendants from a generation-0 element (patriarch).

The generation of new elements leads to siblings ("children") of various generations. Note that the parents are hermaphrodites: only one parent is needed to generate children.

The reproduction or fission process is governed by the widely used 1-irregular rule, which provides a reasonable limit for mesh gradation. If mesh gradation is too severe, the constraints imposed by the coarse elements on their refined neighbors would preclude their full effectiveness. The reason for this is that if a fine set of elements lies adjacent to a coarse element, the velocities of the nodes shared by the two must all be linearly related. Even with the 1-irregular gradation, the adaptivity loses effectiveness when a single fissioned element is surrounded by four unfissioned elements, since then only one <u>new</u> <u>unconstrained</u> node is created. For this reason, nonhermaphroditic generation algorithms which require two <u>adjacent</u> parents to generate 4, 6, or 8 children may prove more effective.

The relationship between families is expressed by the NPTCON (neighboring patriarch connectivity) array. The dimensions of this array are NPATCH × 4, where NPATCH is the number of patriarchs. The columns of the NPTCON array identify the four neighboring patriarchs, so NPTCON (j,i), i = 1 to 4, give the numbers of the four adjacent patriarchs. If side i of a patriarch lies on the boundary of the model, then NPTCON (j,i) = 0.

The following additional arrays are needed:

1. NGENRA(i) = number of ancestor generations for element i.
2. NGENRD(i) = number of descendant generations for element i.
3. NPAREN(i) = the element which is the immediate parent of element i.
4. NSBLNG(j) = a dynamically allocated array which lists all siblings.
5. NCHILD(i) = a pointer array which identifies the starting address of the siblings of element i in the NSBLNG array.

All of the arrays, except the fourth, are of length NELE.

Distinctions among different node types are recorded in the NFLAG(i) array, i = 1 to NNODE, where NNODE is the number of nodes. For slave nodes NFLAG = -1, for boundary nodes NFLAG = 0, for master nodes which are not on a boundary NFLAG = +1. The MASTER array identifies the two nodes which are masters of each slave node. The dimensions of the MASTER array are NNODE × 2. The accelerations, velocities, and displacements are calculated using the average of the values at the two master nodes. It is important to note that this simplified treatment of slave nodes arises from the 1-irregular rule.

Figure 3 summarizes the numbering conventions employed in this data structure.

Rheinboldt and Mesztenyi (1980) use labels for each point (node or element) to determine whether a side of an element borders elements of the same family or not. These labels need not be stored for our data structure. Instead, the position of the element within the sibling group is used to convey this information; that is, sibling 1 translates to Rheinboldt and Mesztenyi's (1980) label (-1, -1), sibling 2 corresponds to (+1, -1), sibling 3 corresponds to (+1, +1), and sibling 4 corresponds to (-1, +1).

The example shown in Figs. 4 and 5 illustrates the role of each of the aforementioned arrays in the data structure. Figure 4 gives the original mesh.

Assume that element 1 has been chosen for fission into elements 5 to 8 by an error criterion. Element 1 is a generation-0 element (patriarch). A patriarch can always be fissioned. The neighboring patriarchs are contained within the NPTCON array.

If side I of element 1 lies on the boundary, NPTCON(5,I) = 0, so a boundary node N (NFLAG(N) = 0) is automatically generated at the midpoint of that side. For the sides of element 1 which border other patriarchs, a test must be performed to ascertain whether slave nodes are already present (NGENRD (NPTCON(5,I)) > 0) or whether new nodes need to be created (NGENRD (NPTCON(5,I)) = 0). If a slave node is present, its node number must be determined via tree travel and the connectivity array, and its status must be upgraded to master node (NFLAG(N) = +1). If a new node must be created, a new node number must be generated.

The new mesh and its associated data structure are shown in Fig. 5.

Now suppose that element 7 in the refined mesh has been chosen for fission by some error criterion. It can be readily observed that the fission of element 7 would result in the violation of the irregular-1 rule. The algorithm determines that element 7 is not suitable for fission in the

following manner. Within the children of parent element 1, element 7 is in the third sibling position. Sides 1 and 4 of sibling 3 border on siblings 2 and 4, respectively. A check of the 1-irregular rule by the fission of element 7 does not need to be done for these two sides. Sides 2 and 3, in this case, border on neighboring families. This is determined by the family tree of element 7 → 3 (sibling position) → +1 +1 (labels). Since the tree is only one entry long, there obviously is no change of sign down the two columns of regularity numbers. Therefore, both sides 2 and 3 border on neighboring families. The families are identified by the NPTCON array, NPTCON(1,2) = 2 and NPTCON(1,3) = 3. These families must have descendants with family trees -1 +1 (labels) → 4 (sibling position) and +1 -1 → 2, respectively. These descendants don't exist. Therefore, fission must be performed on elements 2 and 3 before element 7 can be fissioned.

5. NUMERICAL EXAMPLES

All numerical examples described in this section were performed on a Harris 800 computer in single precision. A single-precision word consists of 11 significant digits (base 10) on this computer.

Since closed-form solutions are not available for nonlinear transient problems, two types of comparisons are used for the adaptive solutions:

1. numerical results obtained by finer meshes;
2. experimental results.

The first example concerns a clamped beam which is impulsively loaded over the center portion as shown in Fig. 6. Using symmetry, half of the beam is modelled by m × n quadrilateral plate elements, with m elements across the 1.2 in. width and n elements over the 5 in. half-span. The x and z components of the translations and rotations about the x and z axes are constrained. The problem is solved using an incremental flexure energy criterion and a single level of refinement.

Figure 7 shows the midspan deflection obtained by two fixed meshes and an 8- to 10-element adaptive mesh. As can be seen, the adaptive mesh is quite close to the 20-element fixed mesh for the first 0.5 msec, and it matches the maximum displacement quite well. Subsequently, it diverges somewhat from the fine-mesh solution.

Figure 8 shows the pattern of mesh adaptivity. The first elements to be fissioned are those beneath the impulsive load; the location of the fissioned elements then moves back and forth between the center and the support, like the hinge in the rigid-plastic solution, and finally fixes itself at the clamped wall.

The profiles of the beam obtained by a fine fixed mesh and the adaptive mesh are compared in Fig. 9. As can be seen, the profiles compare quite

well, except at the final time, 0.49 msec, when the node at the adaptive mesh at x = 3.0 in. deviates markedly.

This beam was resolved with a 2 × 20 fixed mesh and a 16-element adaptive mesh. The midspan deflection is shown in Fig. 10. In this case, the adaptive mesh corresponds very closely with the fixed mesh, even though it required only 40% of the elements. The potential savings in computational resources is even greater, because, in the adaptive mesh, half of the elements could employ a time step twice as large as that used in the fixed mesh.

A more complex example for the adaptive mesh is provided by the cylindrical panel problem shown in Fig. 11. An initial velocity of 5650 in/sec is applied to the 3.08 in. × 10.205 area indicated in Fig. 11. The panel is simply supported at its ends and clamped at the sides. An Ilyushin plasticity model, which is expressed in terms of the resultant moments and membrane forces, m_{ij} and σ_{ij}, is used in the computation.

The problem was solved with both multi-level and two-level adaptivity (patriarchs were allowed to fission once).

We first give the results for two-level adaptivity.

Two adaptive meshes were used in the two-level computation: a 96-element mesh based on a 4 × 8 mesh of molecules, and a 218-element mesh based on an 8 × 16 mesh of molecules. The results are compared to uniform fixed meshes with 32, 96, 128, 218, and 512 elements.

The displacement time histories for the coarse adaptive mesh are compared to three of the fixed-mesh results in Figs. 12 and 13 at points A (z = -6.28 in.) and B (z = -9.42 in.) which are indicated in Fig. 11. Remarkably, the 53-element adaptive result almost coincides with the 128-element fixed-mesh result for the first 0.4 msec. Subsequently, the results

of the two meshes deviate somewhat, and the adaptive results become slightly rough, which is caused by excessive churning of the fission-fusion process. Note that the fixed-mesh results with fewer elements deviate substantially from the finest fixed-mesh results.

The displacements for the fine adaptive mesh are compared to the fixed meshes in Figs. 14 and 15 at points A and B, respectively. Here the 218-element adaptive mesh corresponds quite closely with the 512-element uniform fixed mesh and exhibits marked improvement over a 200-element fixed mesh.

Deformed mesh plots for the finer adaptive mesh are shown at various times in Fig. 16. Here the incremental energy is used for the fission-fusion criterion. It can be seen that after 0.0125 msec, the crown settles downward like a plateau and the fissioning process migrates laterally towards the line where the curvature is maximum. During this time, the crown moves down in a frozen plateau-like state. After that, the crown develops a convex curvature when viewed from above, and the elements in the crown are again fissioned. The end of the simulation again exhibits churning of fission-fusion, which is a tendency that needs to be fixed: it is probably due to the fact that the incremental work is quite small in the later stages because most of the deformation has taken place, so the incremental work in molecules is quite uniformly distributed, allowing the fission-fusion process to be triggered by small oscillations in the solution.

Experimental results have been obtained for this shell by Morino, Leech, and Witmer (1971), who report a maximum deflection of 1.24 in. at point A. The finest fixed and adaptive meshes yield maximum deflections of 1.20 and 1.17 in., respectively. These results show that even two-level adaptivity is quite successful.

The deformed profiles are shown in Figs. 17 and 18 for the 512-element fixed mesh and the 218-element adaptive mesh. The development of a hinge line at about x = 2.0 in. and the attendant fission process are quite clearly seen in Fig. 17. Figure 18 shows a cross section in the y-z plane of symmetry. The fusion process which takes place while the crown is moving like a flat plateau, followed by the fission which develops when the crown curves, is quite clearly seen.

The results for the multi-level adaptivity solution of the cylindrical panel problem are given next. The interelement angle criterion is used in this case.

The deformed meshes are shown in Fig. 19. It should be noted that initially the largest element rotations occur for those elements on the near end (z = 0) of the shell. This is a clamped support, and a hinge line forms immediately. The first few mesh plots indicate that the elements are indeed being reallocated to this region. Later in the simulation, as the hinge line forms at x = 2.0 in., most of the refinement focuses there because little additional deformation occurs. In contrast to the results based on the incremental energy criterion, all elements in the center of the panel are fused at the end.

A comparison between calculated displacement time histories at points A and B, using adaptive and fixed meshes and experimental results, is given in Figs. 20 and 21. The tremendous improvement which is attainable with multi-level refinement is quite clear. The results for the peak displacement of node A correspond almost exactly with the experiment.

In this multi-level solution, three descendant generations were used. Fission-fusion judgments were made every 40 time steps, and since the duration of the simulation was 0.6 msec, it occurred 86 times (no judgement

was made until the 80th step). Fission or fusion was performed only when indicated by two consecutive judgments.

The third example is a hollow, cylindrical column which is subjected to a compressive axial load. This problem is of interest because it exhibits both global and local buckling, the latter resulting in buckling of the cross section. Numerical results and experimental results are reported for this problem by Kennedy, Belytschko, and Lin (1986). The problem parameters are given in Table 1.

The cylinder is loaded by prescribing an upward velocity of 500 in/sec to the bottom nodes of the model, with the top fixed. To trigger the lateral buckling mode, an imperfection given by

$$\Delta x = 0.01 \sin \frac{2\pi z}{\ell}$$

where ℓ is the length of the column and z is the coordinate along the axis of the column, is added to the x-coordinate of all nodes.

The problem is solved with multi-level adaptivity and the angle error criterion. The pattern of adaptivity is shown in Fig. 22. Initially, the fission process is only one level and occurs at the eventual extrema of the buckling wave. The fission process then coalesces at the nodes of the lateral buckling mode, where they attain a higher level. Some fission also takes place at the compressive buckles at the top and bottom of the column. The displacements of two points in the adaptive mesh are compared to corresponding points in a finer fixed mesh in Fig. 23. The results show good agreement.

6. CONCLUSIONS

An adaptive procedure based on an h-scheme has been developed for the nonlinear transient analysis of shells. Refinement is implemented through fission of an element into four elements, and coarsening, through fusion of four elements into one. Suitable criteria for fission and fusion and the formulation of the fission and fusion processes are also described.

Two criteria have been found useful for the bilinear quadrilateral elements commonly used in transient analysis by explicit time integration:

1. the incremental internal work criterion;
2. the relative angle criterion, which is a measure of the deviation of the bilinear surface from the Kirchhoff-Love surface associated with the nodal orientations.

The angle criterion appears to be the more effective of the two, since it is readily applicable to multi-level adaptivity. The incremental energy criterion requires arbitrary parameters when extended to multi-levels, since the incremental work performed depends on element size.

It would be desirable to supplement the angle criterion since deviation of the bilinear approximation is not the only source of errors. For example, another source of errors is the one-point quadrature and the perturbation hourglass control. To reduce errors, those elements which deform primarily in the hourglass mode should be refined. Similarly, a criterion which identifies errors due to high stress gradients would be desirable. However, such supplementary criteria have the drawback that weights must be assigned to these different criteria in using them for adaptivity. A unified approach which accounts for all of these errors would therefore be desirable.

To avoid excessive churning of the fission-fusion process, time delays had to be incorporated in the judgment process. Thus, fission and fusion are executed only when indicated by two or more consecutive judgments. Nevertheless, churning becomes a problem with the incremental work criterion in the later stages of impulsively loaded problems when the work on the system decreases.

The h-adaptive procedure is limited in its ability to focus on the subdomains of maximum deformation by the fact that the parent element configuration is fixed. Therefore, hinge lines which occur at angles relative to the mesh lines may not be captured effectively. However, the h-adaptive procedure appears to be the best compromise between simplicity and effectiveness in the solution of nonlinear structures by explicit methods.

The results we have obtained show that these adaptive schemes are capable of achieving substantial improvements in accuracy for a given computational effort. Generally, an adaptive mesh is capable of achieving the same level of accuracy as a fixed mesh with less than half of the computational resources. The fission process tends to take place in the subdomains where the maximum deformation occurs.

REFERENCES

R. E. Bank and A. H. Sherman (1980). "A Refinement Algorithm and Dynamic Data Structure for Finite Element Meshes", Technical Report 166, Center for Numerical Analysis, The University of Texas at Austin, Austin, TX.

R. E. Bank, A. H. Sherman, and A. Weiser (1983). "Refinement Algorithms and Data Structures for Regular Local Mesh Refinement", in IMACS Transactions on Scientific Computation (10th IMACS World Congress on Systems Simulation and Scientific Computation, Montreal, Canada), ed. R. S. Stepleman, M. Carver, R. Peskin, W. F. Ames, and R. Vichnevetsky, IMACS/North-Holland Publishing Company, Amsterdam, pp. 3-17.

T. Belytschko, J. I. Lin, and C.-S. Tsay (1984). "Explicit Algorithms for the Nonlinear Dynamics of Shells", Computer Methods in Applied Mechanics and Engineering, 42, 225-251.

T. Belytschko and R. Mullen (1978). "On Dispersive Properties of Finite Element Solutions", in Modern Problems in Elastic Wave Propagation, ed. J. Miklowitz and J. D. Achenbach, Wiley, New York, pp. 67-82.

P. Devloo, J. T. Oden, and T. Stroubelis (1987). "Implementation of an Adaptive Refinement Technique for the SUPG Algorithm", Computational Methods in Applied Mechanics and Engineering, 61, 339-358.

R. E. Ewing (1986). "Adaptive Mesh Refinements in Large-Scale Fluid Flow Simulations", in Accuracy Estimates and Adaptive Refinements in Finite Element Computations, ed. I. Babuska, O. C. Zienkiewicz, R. Gago, and A. Oliveira, Wiley, New York.

J. O. Hallquist and D. J. Benson (1986). "DYNA3D User's Manual (Nonlinear Dynamic Analysis of Structures in Three Dimensions)", Report UCID-19592, Revision 2, University of California, Lawrence Livermore National Laboratory, Livermore, CA.

J. M. Kennedy, T. Belytschko, and J. I. Lin (1986). "Recent Developments in Explicit Finite Element Techniques and Their Application to Reactor Structures", Nuclear Engineering and Design, 97(1), 1-24.

L. Morino, J. W. Leech, and E. A. Witmer (1971). "An Improved Numerical Calculation Technique for Large Elastic-Plastic Transient Deformations of Thin Shells: Part 2 - Evaluation and Applications", Journal of Applied Mechanics, 38(2), 429-436.

A. K. Noor and I. Babuska (1987). "Quality Assessment and Control of Finite Element Solutions", Finite Elements in Analysis and Design, 3(1), 1-26.

J. T. Oden and L. Demkowicz (1988). "Advances in Adaptive Improvements: A Survey of Adaptive Finite Elements in Computational Mechanics", in State of the Art Surveys in Computational Mechanics, ed. A. K. Noor et al, ASME, New York, in press.

W. C. Rheinboldt and C. K. Mesztenyi (1980). "On a Data Structure for Adaptive Finite Element Mesh Refinements", ACM Transactions on Mathematical Software, 6, 166-187.

Table 1

Specification of Column Buckling Problem

Column diameter	$D = 13.0$ in.
Wall thickness	$t = 1.0$ in.
Column length	160.0 in.

Material Properties

Young's modulus	$E = 2.8 \times 10^{7}$ psi
Density	$\rho = 8.31 \times 10^{-4}$ lb-sec^2/in^4
Poisson's ratio	$\nu = 0.25$
Yield stress	$\sigma_\gamma = 35000$ psi

Prescribed displacement loading

$\dot{\delta} = 500$ in/sec

Plastic behavior is modelled by a ten-segment piecewise linear approximation to the stress-strain curve and the Von Mises yield criterion.

	Plastic moduli (psi)	Plastic stresses (psi)
(1)	6.60×10^5	4.75×10^4
(2)	4.50×10^5	5.65×10^4
(3)	4.00×10^5	6.45×10^4
(4)	2.75×10^5	7.00×10^4
(5)	2.50×10^5	7.50×10^4
(6)	2.25×10^5	7.95×10^4
(7)	2.20×10^5	8.35×10^4
(8)	1.75×10^5	8.70×10^4
(9)	1.50×10^5	9.00×10^4
(10)	1.25×10^5	1.15×10^6

LIST OF FIGURES

Figure 1. Fusion and fission.

Figure 2. Interface between a fused and a fissioned molecule on a curved surface.

Figure 3. Conventions for the data structure.

Figure 4. The data structure for the initial coarse mesh.

Figure 5. The data structure after fission of paterfamilia element 1.

Figure 6. Impulsively loaded clamped beam. Young's modulus E = 10.4×10^6 psi; density $\rho = 2.61 \times 10^{-4}$ lb-sec^2/in^4; Poisson's ratio $\nu = 0.3$; yield stress $\sigma = 41400$ psi; plastic modulus $E_p = 0$ psi; initial velocity = 5000 in/sec; thickness = 0.125 in.

Figure 7. Centerpoint deflection of the clamped beam.

Figure 8. Undeformed and deformed plots for the clamped beam with a 10-element adaptive mesh.

Figure 9. Deformed cross-sectional profile of the clamped beam with 2 × 10 mesh.

Figure 10. Centerpoint deflection of the clamped beam with finer mesh.

Figure 11. Impulsively loaded cylindrical panel. Young's modulus E = 10.5×10^6 psi; density $\rho = 2.5 \times 10^{-4}$ lb-sec^2/in^4; Poisson's ratio $\nu = 0.33$; yield stress $\sigma = 44000$ psi; plastic modulus E_p = 0 psi; radius R = 2.9375 in.

Figure 12. Displacement time history for node A of the cylindrical panel with coarse mesh and two-level adaptivity.

Figure 13. Displacement time history for node B of the cylindrical panel with coarse mesh and two-level adaptivity.

Figure 14. Displacement time history for node A of the cylindrical panel with finer mesh and two-level adaptivity.

Figure 15. Displacement time history for node B of the cylindrical panel with finer mesh and two-level adaptivity.

Figure 16. Undeformed and deformed plots for the cylindrical panel with fine adaptive mesh and two-level adaptivity.

Figure 17. Deformed cross-sectional profiles of the cylindrical panel with a fine mesh and two-level adaptivity in an x-y plane passing through node A.

Figure 18. Deformed cross-sectional profiles of the cylindrical panel with a fine mesh and two-level adaptivity in a y-z plane passing through nodes A and B.

Figure 19. Deformed meshes for the cylindrical panel with multi-level adaptivity.

Figure 20. Displacement time history of node A of the cylindrical panel with multi-level adaptivity.

Figure 21. Displacement time history of node B of the cylindrical panel with multi-level adaptivity.

Figure 22. Deformed adaptive meshes for the cylindrical column with multi-level adaptivity.

Figure 23. Displacement time histories for two points of the cylindrical column.

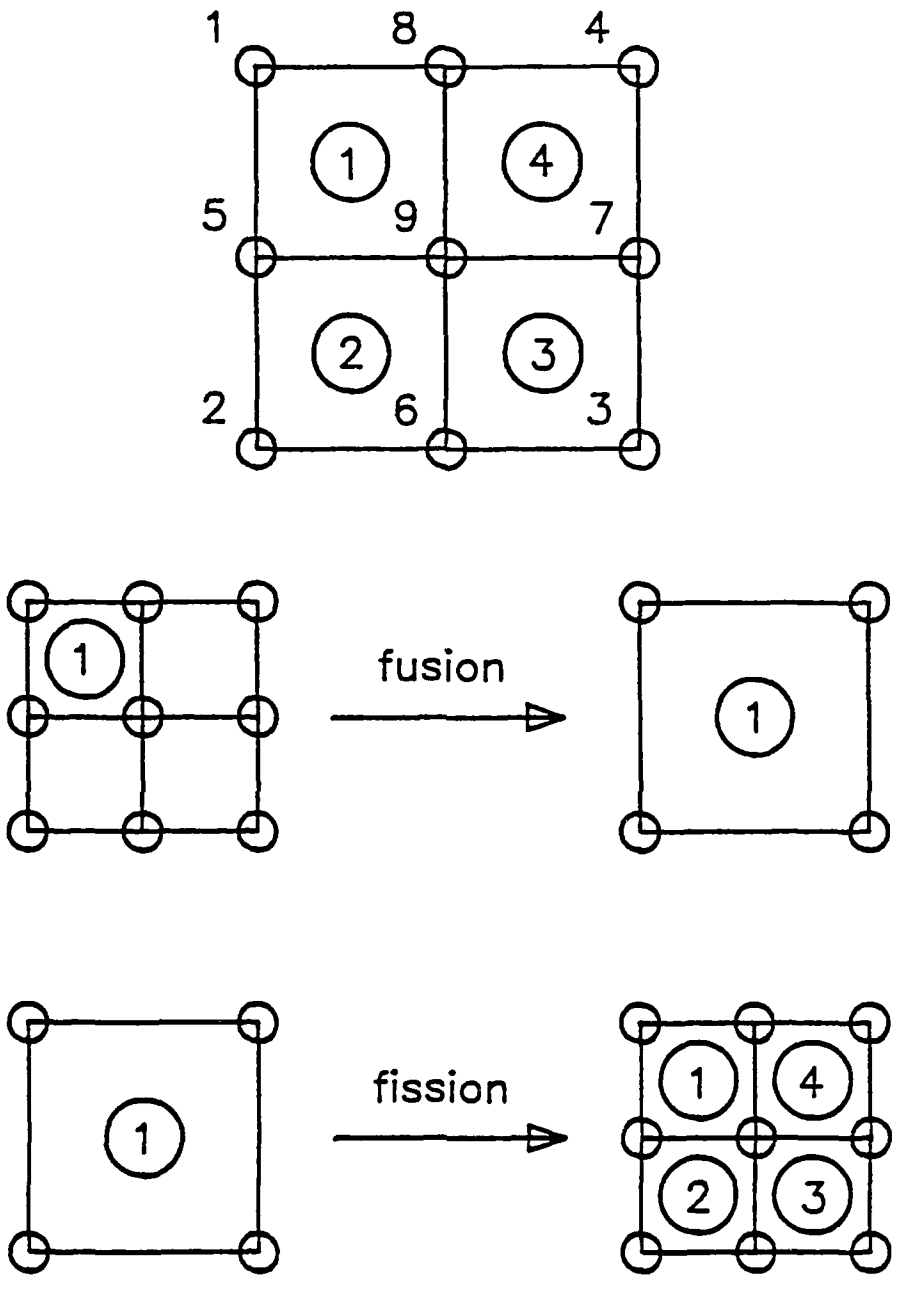

Figure 1

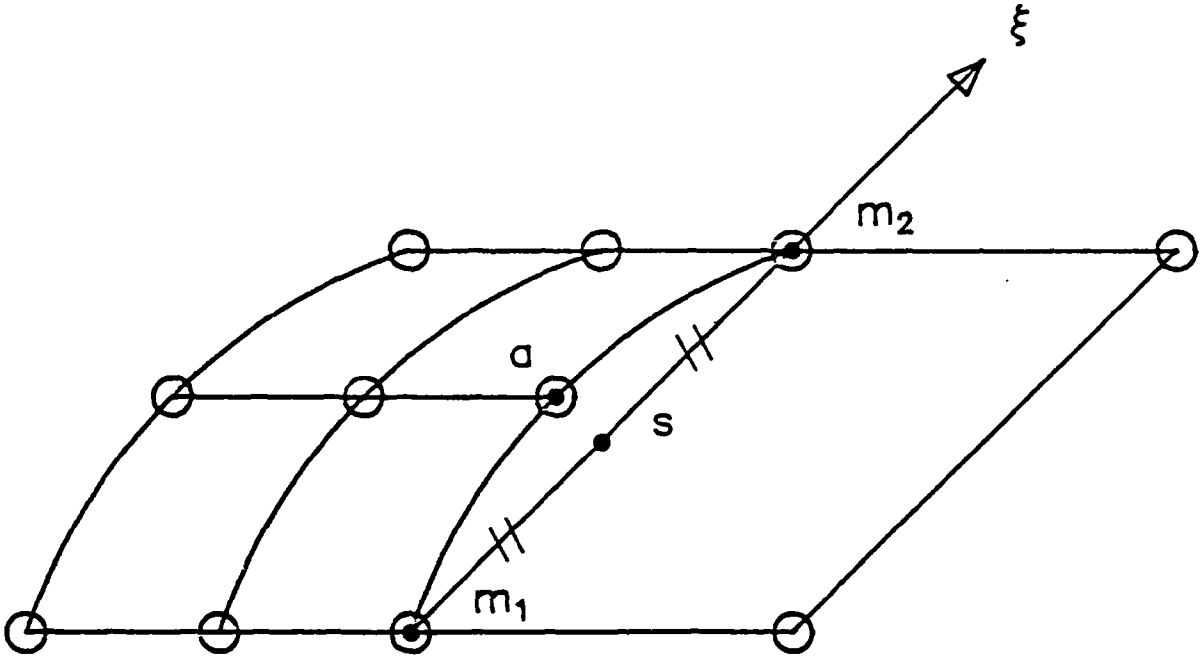

Figure 2

For any Element:

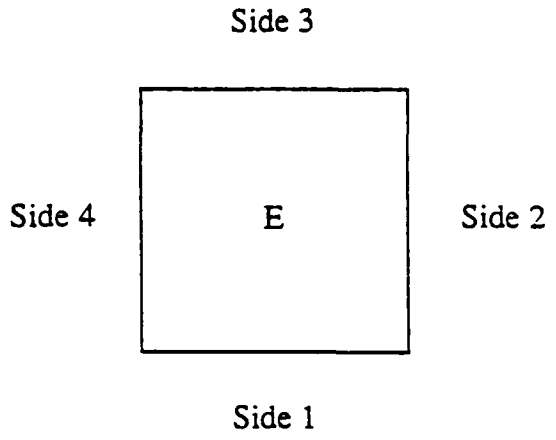

For any Sibling Group:

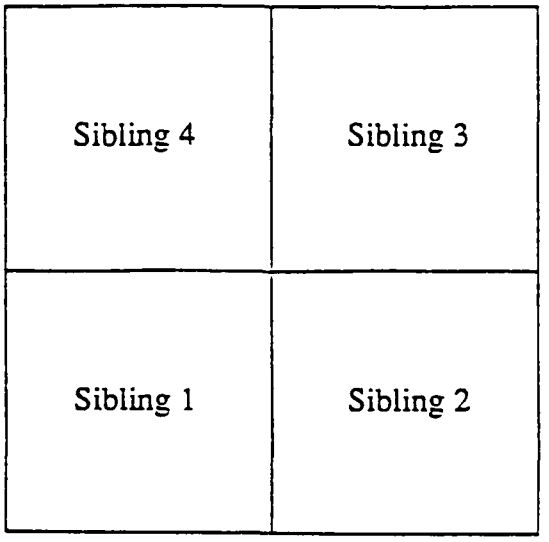

For any Patriarch:

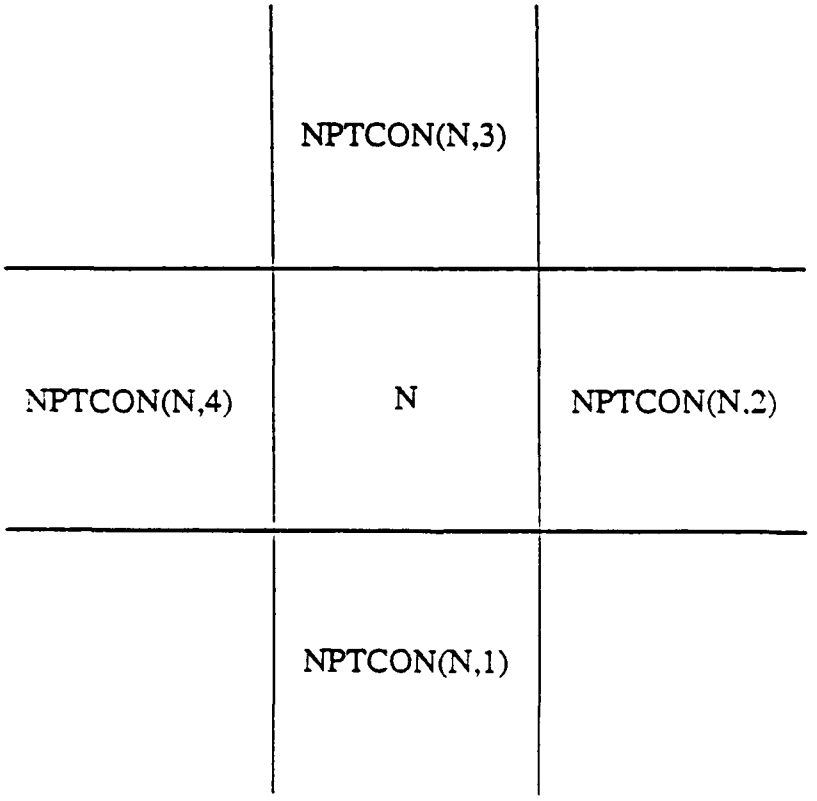

Figure 3

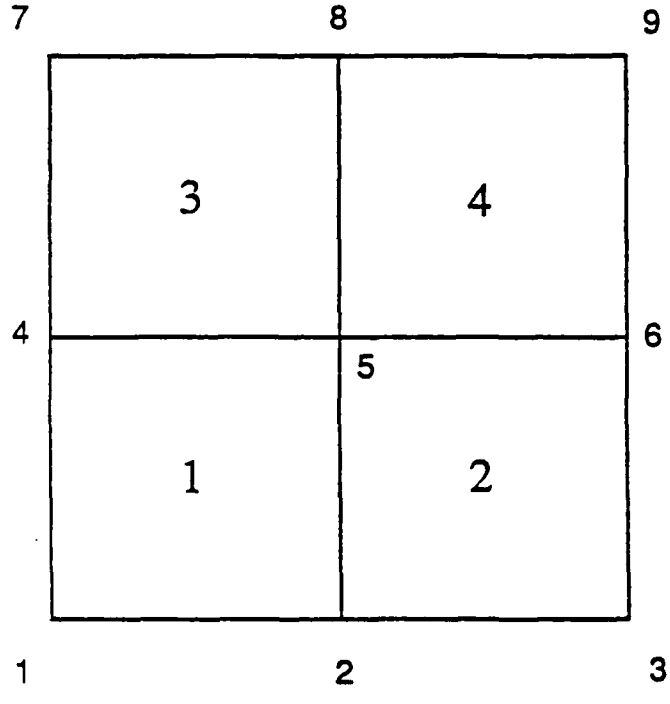

NPATCON

1)	0	2	3	0
2)	0	0	4	1
3)	1	4	0	0
4)	2	0	0	3

NSBLNG

1)	1	0	0	0
2)	2	0	0	0
3)	3	0	0	0
4)	4	0	0	0

	NFLAG		MASTER
1)	0	0	0
2)	0	0	0
3)	0	0	0
4)	0	0	0
5)	+1	0	0
6)	0	0	0
7)	0	0	0
8)	0	0	0
9)	0	0	0

	NODES				NGENRA	NGENRD	NPAREN	NCHILD
1)	1	2	5	4	0	0	0	0
2)	2	3	6	5	0	0	0	0
3)	4	5	8	7	0	0	0	0
4)	5	6	9	8	0	0	0	0

Figure 4

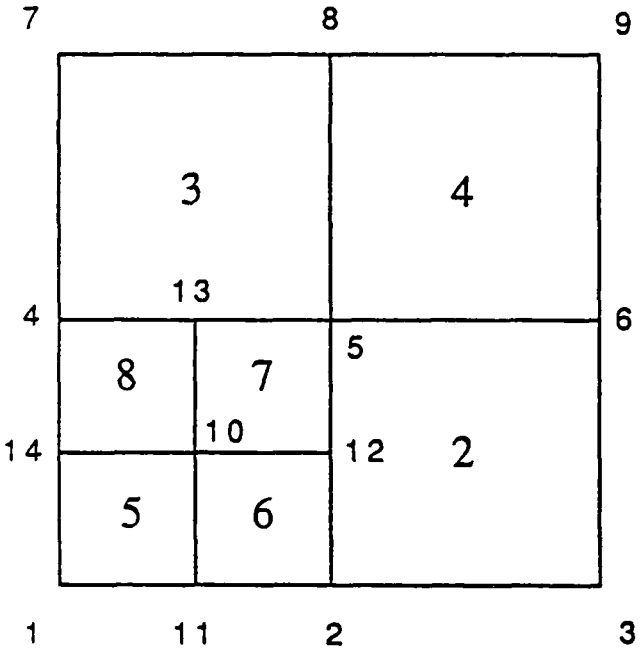

NPATCON

1)	0	2	3	0
2)	0	0	4	1
3)	1	4	0	0
4)	2	0	0	3

NSBLNG

1)	1	0	0	0
2)	2	0	0	0
3)	3	0	0	0
4)	4	0	0	0
5)	5	6	7	8

	NFLAG		MASTER
1)	0	0	0
2)	0	0	0
3)	0	0	0
4)	0	0	0
5)	+1	0	0
6)	0	0	0
7)	0	0	0
8)	0	0	0
9)	0	0	0
10)	+1	0	0
11)	0	0	0
12)	-1	2	5
13)	-1	5	4
14)	0	0	0

	NODES				NGENRA	NGENRD	NPAREN	NCHILD
1)	1	2	5	4	0	1	0	5
2)	2	3	6	5	0	0	0	0
3)	4	5	8	7	0	0	0	0
4)	5	6	9	8	0	0	0	0
5)	1	11	10	14	1	0	1	0
6)	11	2	12	10	1	0	1	0
7)	10	12	5	13	1	0	1	0
8)	14	10	13	4	1	0	1	0

Figure 5

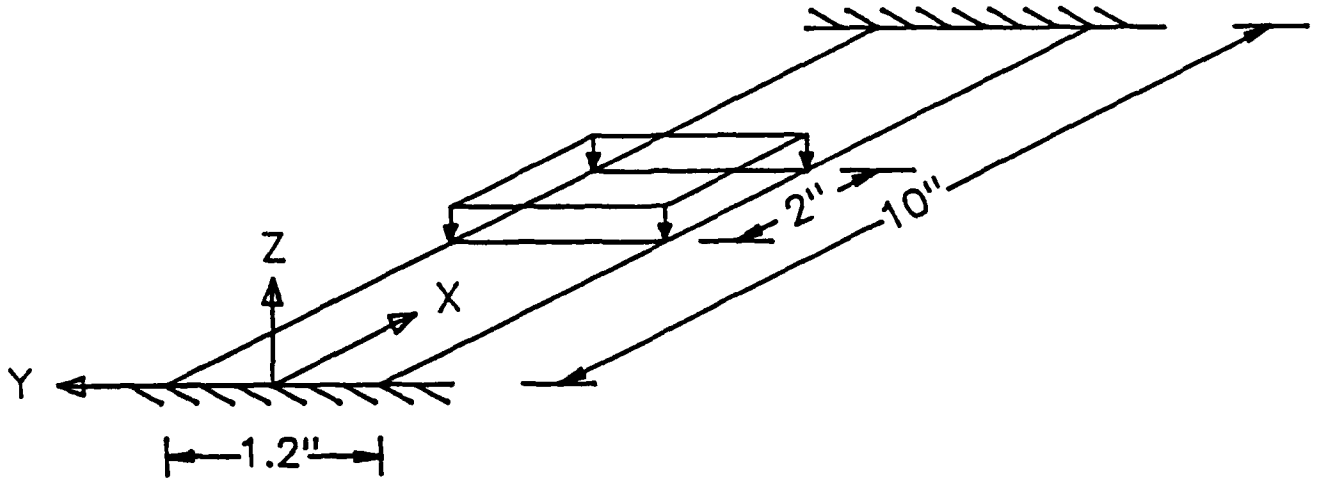

Figure 6

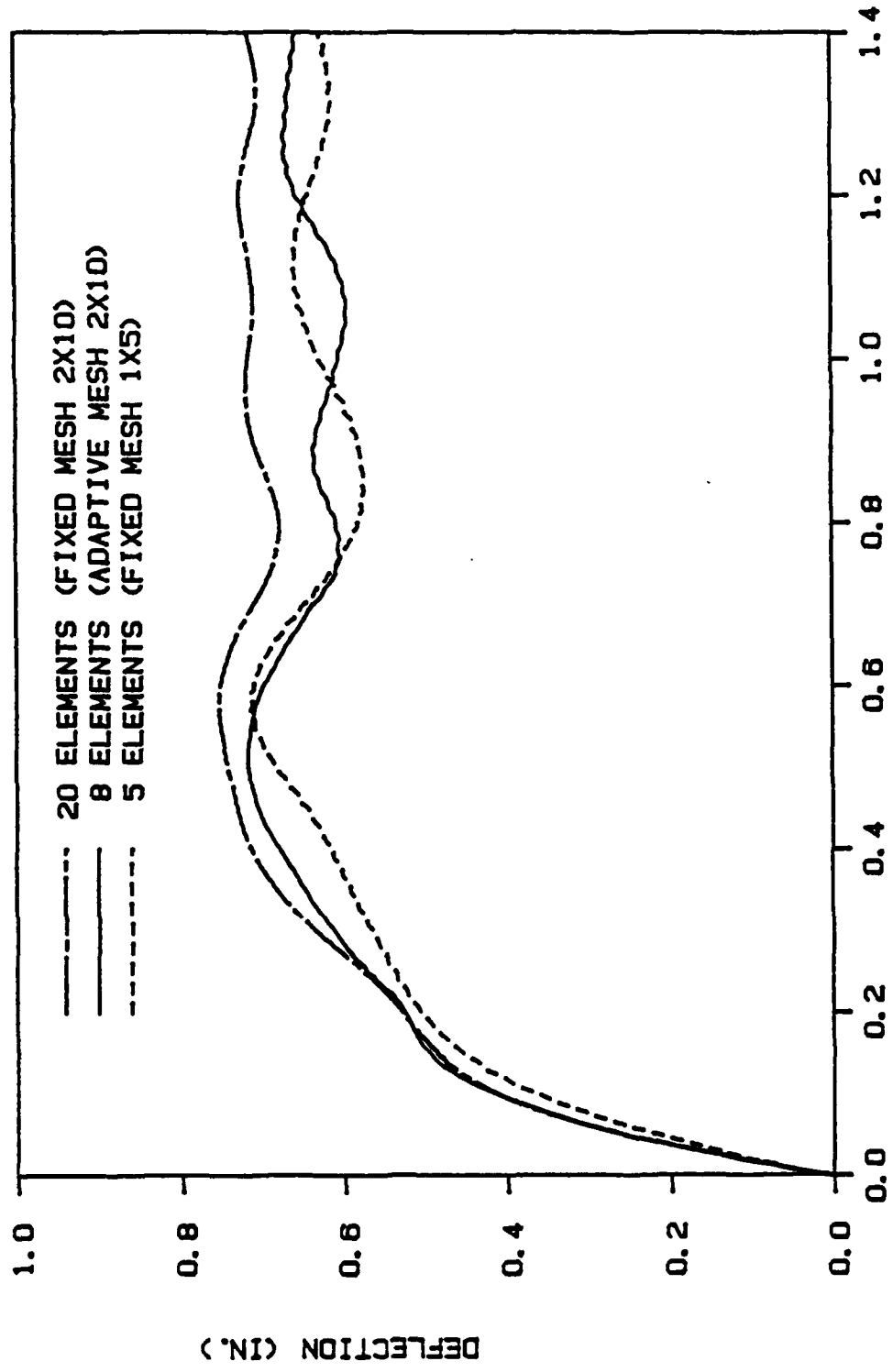
20 ELEMENTS (FIXED MESH 2X10)
8 ELEMENTS (ADAPTIVE MESH 2X10)
5 ELEMENTS (FIXED MESH 1X5)
DEFLECTION (IN.)
1.0
0.8
0.6
0.4
0.2
0.0
0.0
0.2
0.4
0.6
0.8
1.0
1.2
1.4
TIME (MSEC.)

Figure 7

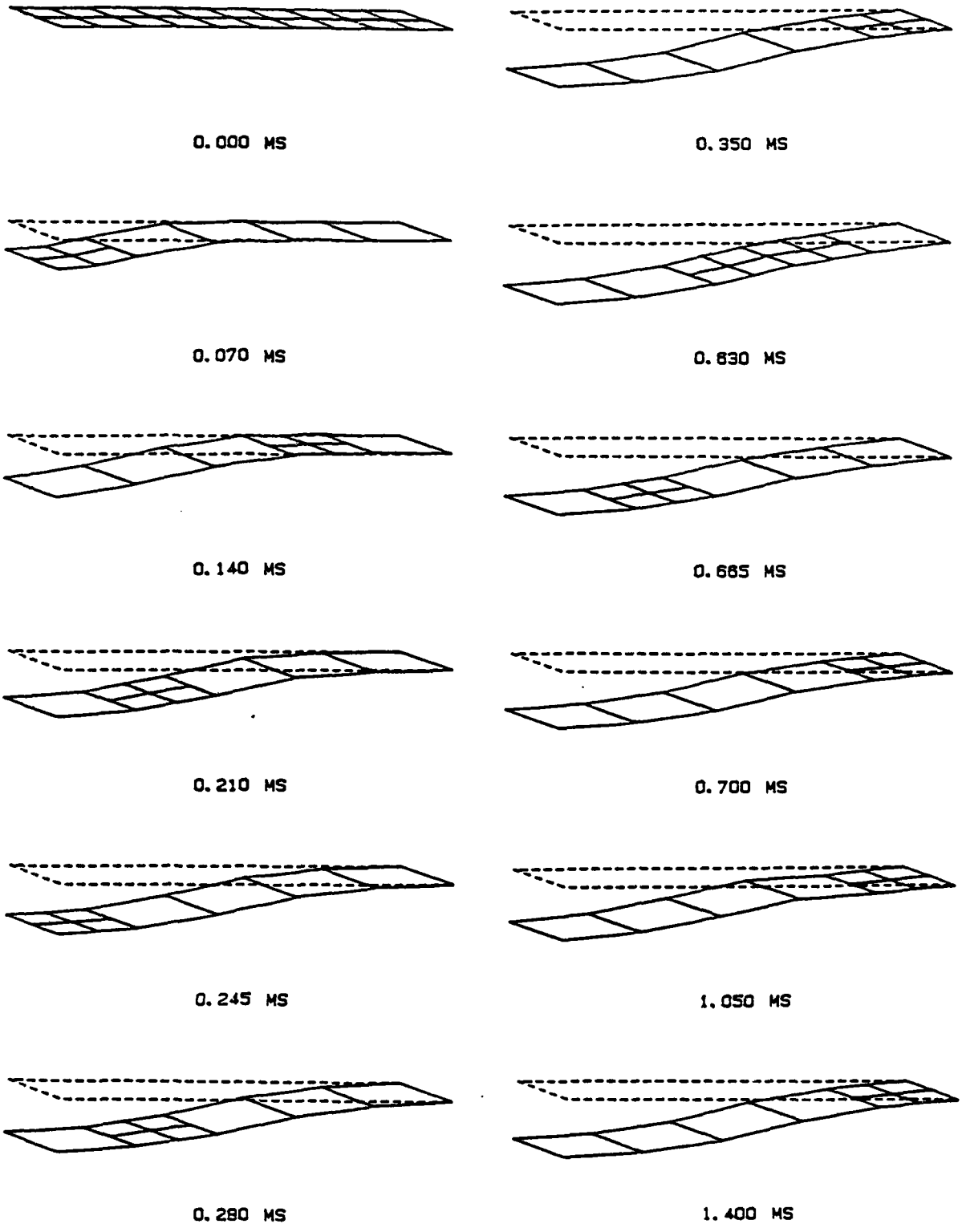
0.000 MS
0.350 MS
0.070 MS
0.630 MS
0.140 MS
0.665 MS
0.210 MS
0.700 MS
0.245 MS
1.050 MS
0.280 MS
1.400 MS

Figure 8

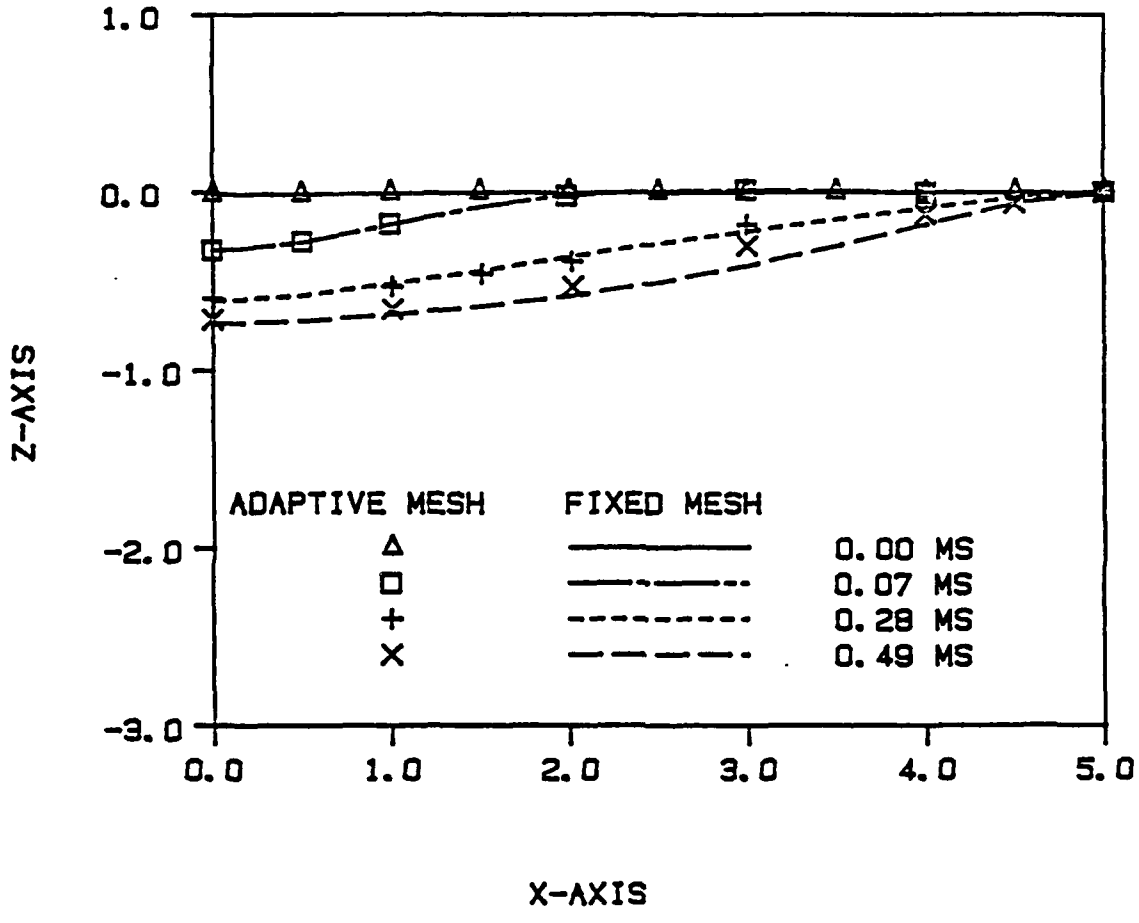
1.0
0.0
-1.0
-2.0
-3.0
Z-AXIS
0.0
1.0
2.0
3.0
4.0
5.0
X-AXIS
ADAPTIVE MESH
FIXED MESH
0.00 MS
0.07 MS
0.28 MS
0.49 MS

Figure 9

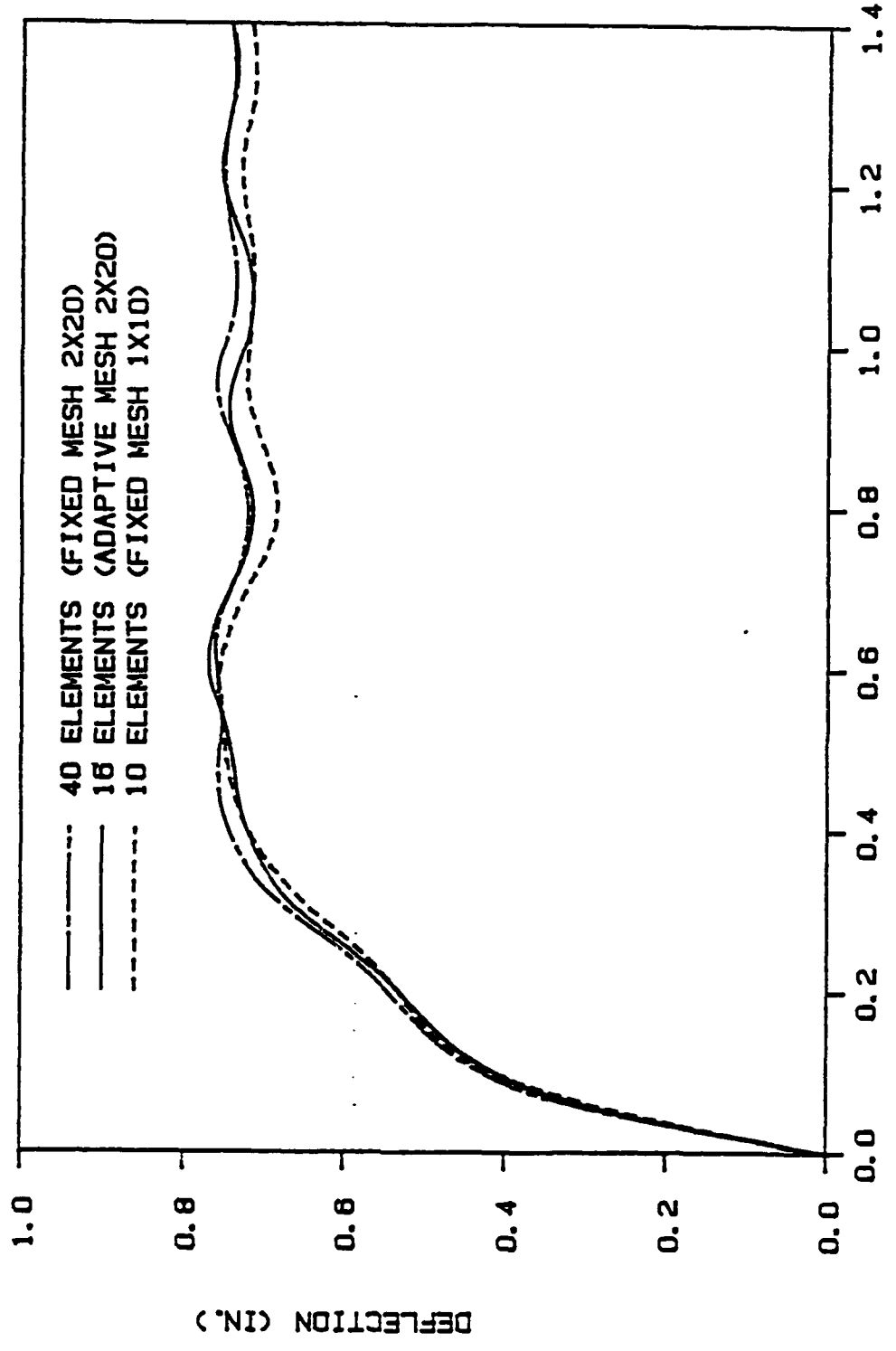
40 ELEMENTS (FIXED MESH 2X20)
16 ELEMENTS (ADAPTIVE MESH 2X20)
10 ELEMENTS (FIXED MESH 1X10)
DEFLECTION (IN.)
TIME (MSEC.)
0.0
0.2
0.4
0.6
0.8
1.0
1.2
1.4

Figure 10

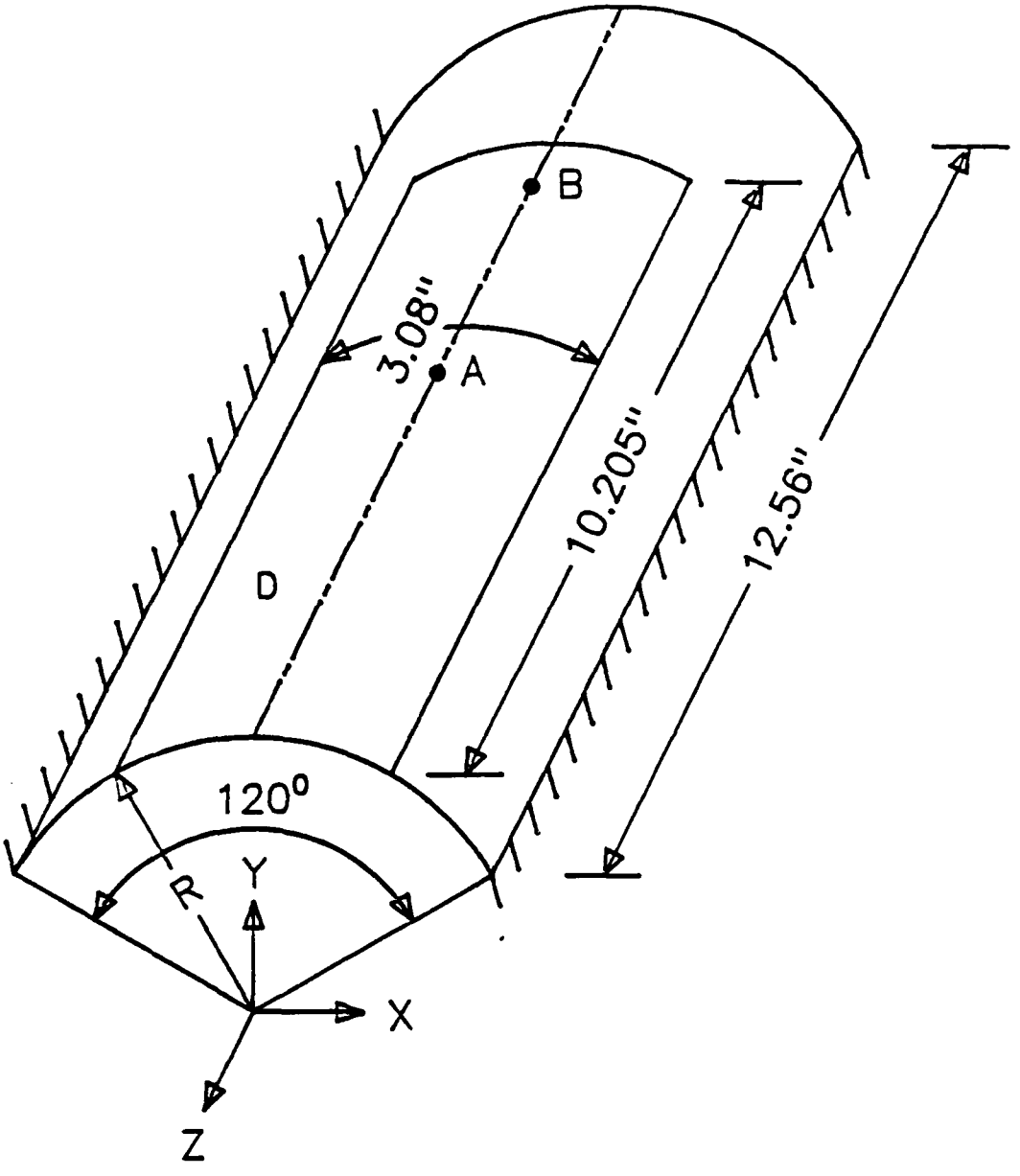

Figure 11

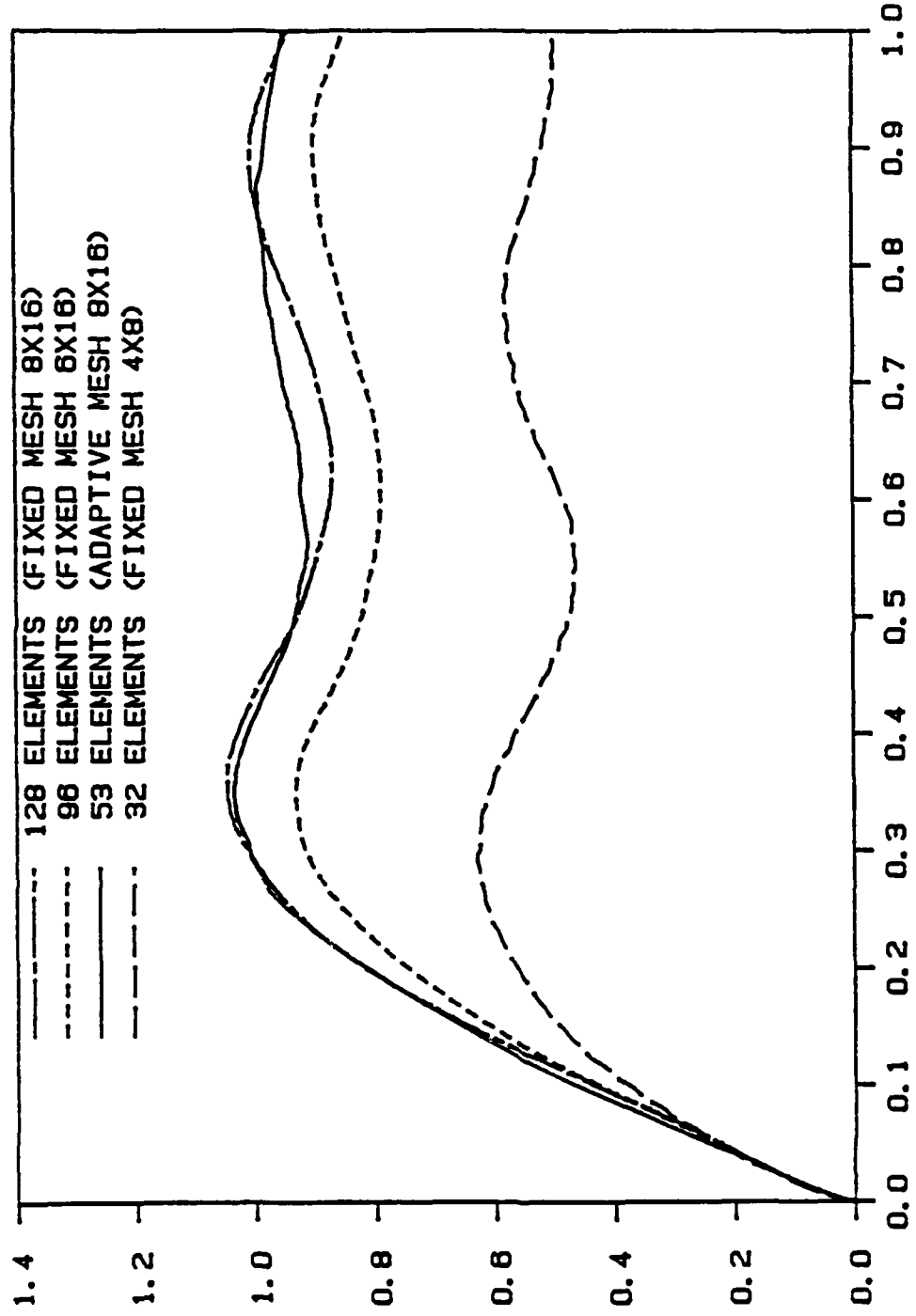
128 ELEMENTS (FIXED MESH 8X16)
98 ELEMENTS (FIXED MESH 6X16)
53 ELEMENTS (ADAPTIVE MESH 8X16)
32 ELEMENTS (FIXED MESH 4X8)
DEFLECTION AT A (IN.)
TIME (MSEC.)
0.0
0.2
0.4
0.6
0.8
1.0
1.2
1.4
0.1
0.3
0.5
0.7
0.9

Figure 12

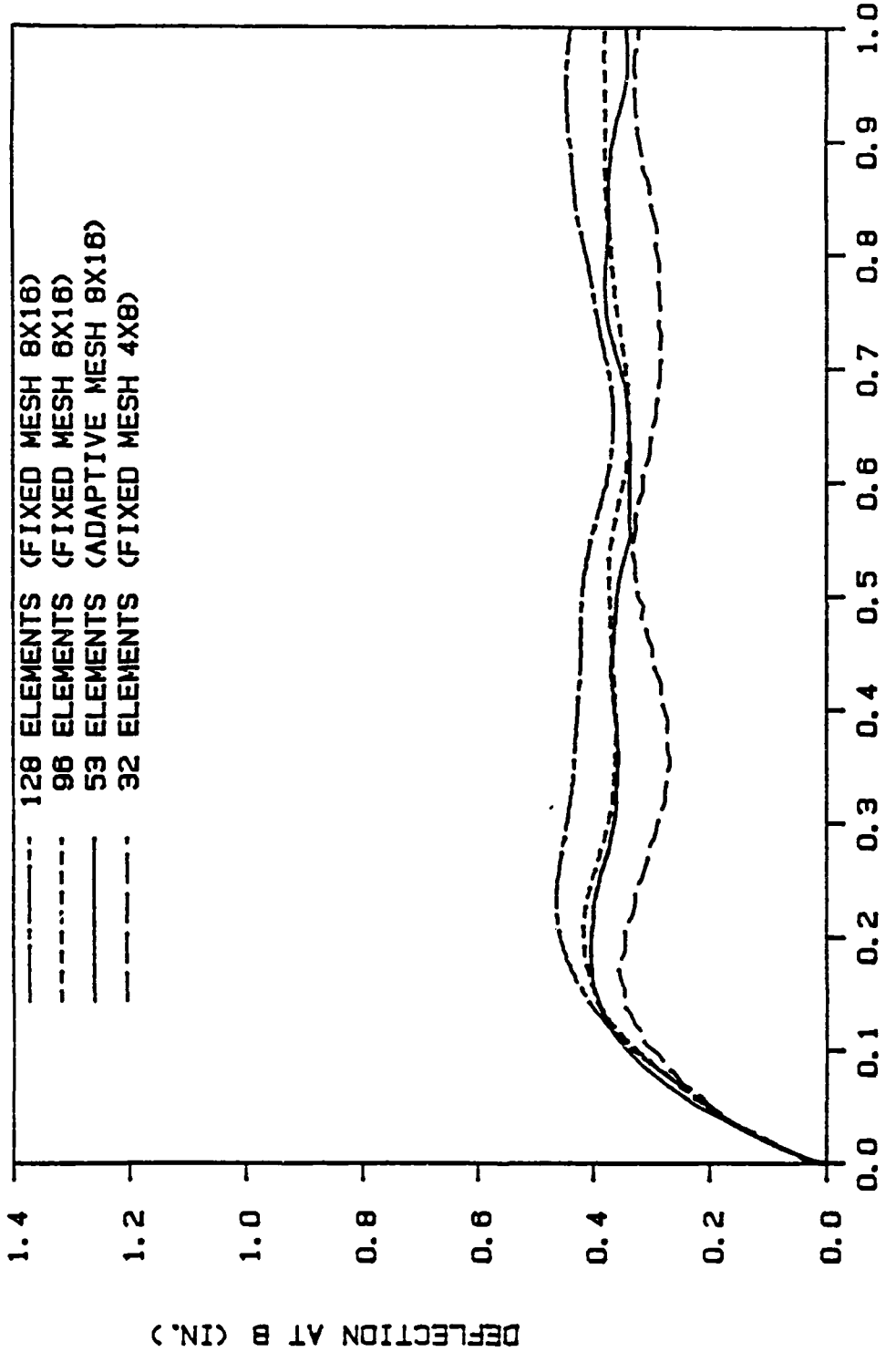
128 ELEMENTS (FIXED MESH 8X16)
96 ELEMENTS (FIXED MESH 6X16)
53 ELEMENTS (ADAPTIVE MESH 8X16)
32 ELEMENTS (FIXED MESH 4X8)
DEFLECTION AT B (IN.)
TIME (MSEC.)
0.0
0.2
0.4
0.6
0.8
1.0
1.2
1.4
0.0
0.1
0.2
0.3
0.4
0.5
0.6
0.7
0.8
0.9
1.0

Figure 13

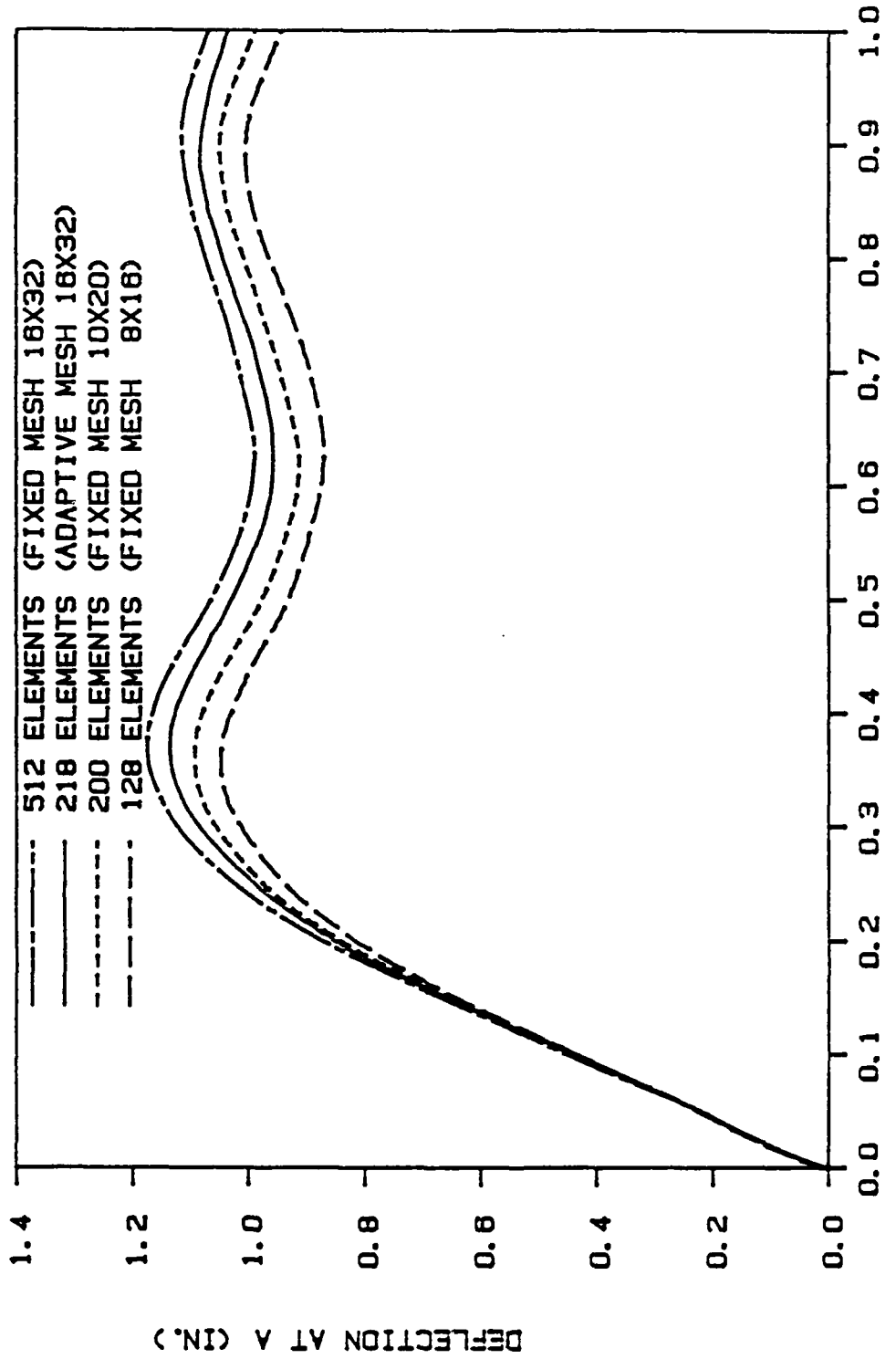
512 ELEMENTS (FIXED MESH 16X32)
218 ELEMENTS (ADAPTIVE MESH 16X32)
200 ELEMENTS (FIXED MESH 10X20)
128 ELEMENTS (FIXED MESH 8X16)
DEFLECTION AT A (IN.)
TIME (MSEC.)
0.0
0.2
0.4
0.6
0.8
1.0
1.2
1.4
0.1
0.3
0.5
0.7
0.9

Figure 14

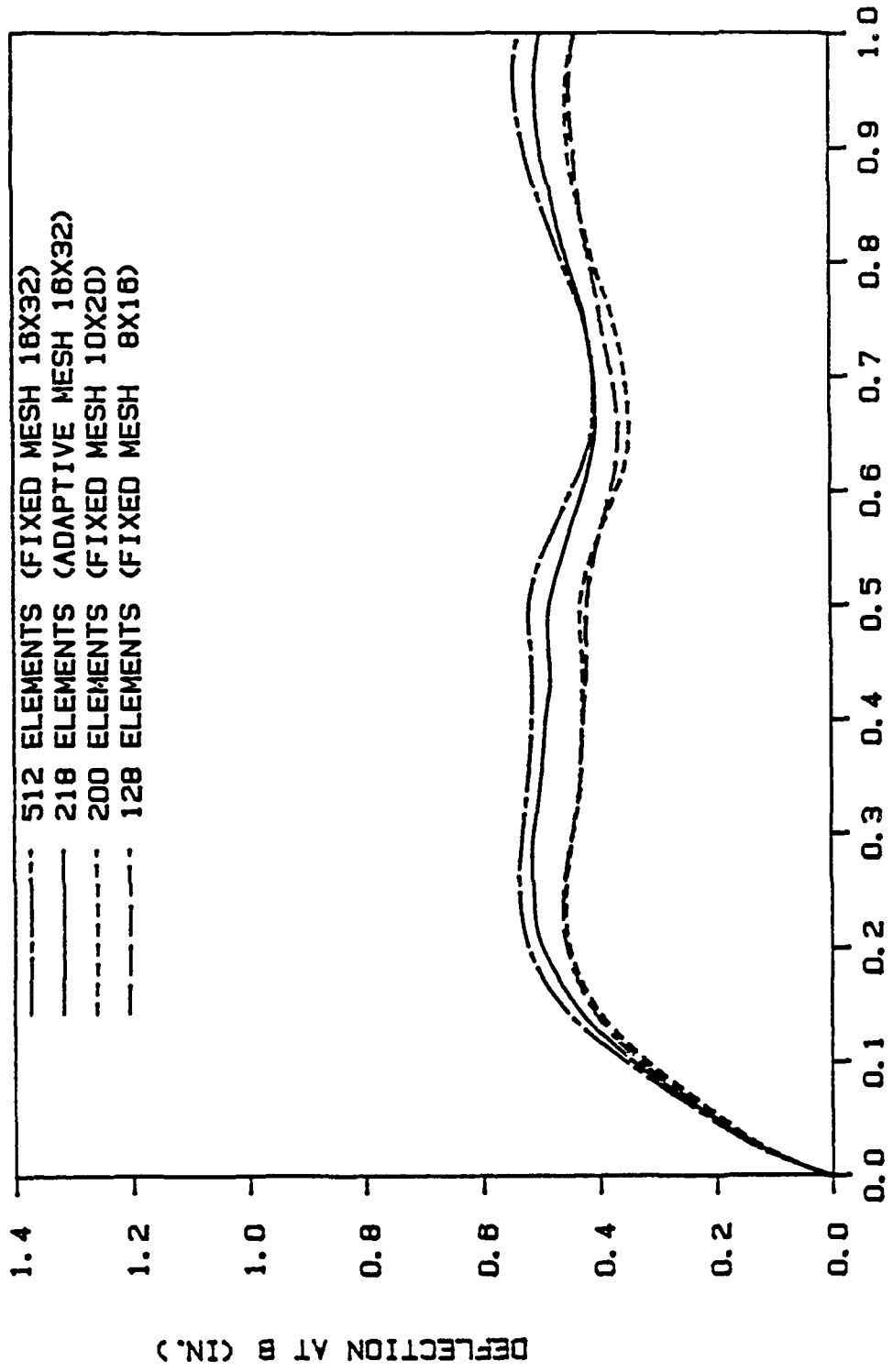
512 ELEMENTS (FIXED MESH 16X32)
218 ELEMENTS (ADAPTIVE MESH 16X32)
200 ELEMENTS (FIXED MESH 10X20)
128 ELEMENTS (FIXED MESH 8X16)
DEFLECTION AT B (IN.)
TIME (MSEC.)
0.0
0.2
0.4
0.6
0.8
1.0
1.2
1.4
0.1
0.3
0.5
0.7
0.9

Figure 15

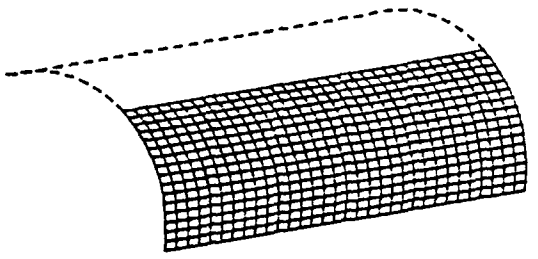

0.000 MS

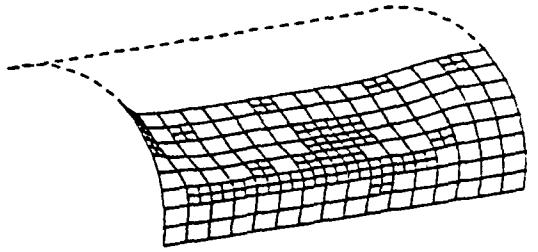

0.100 MS

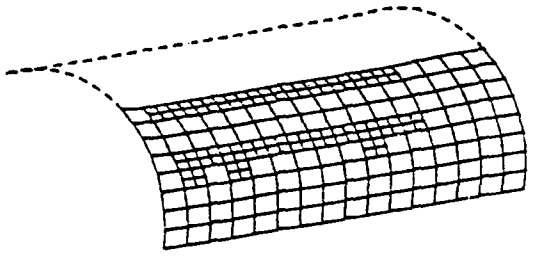

0.0125 MS

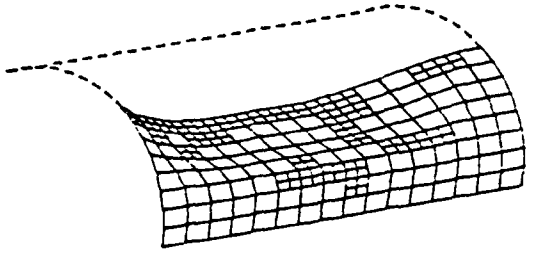

0.200 MS

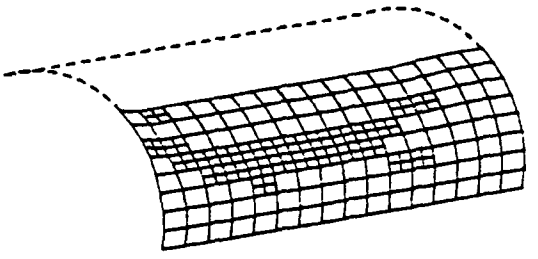

0.025 MS

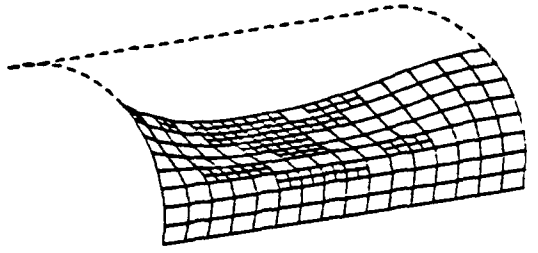

0.250 MS

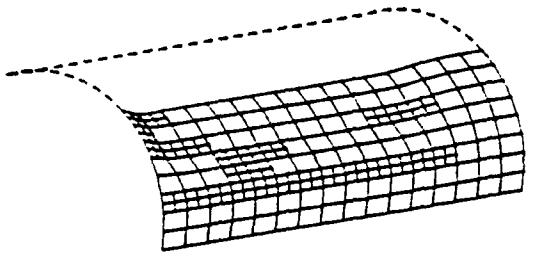

0.050 MS

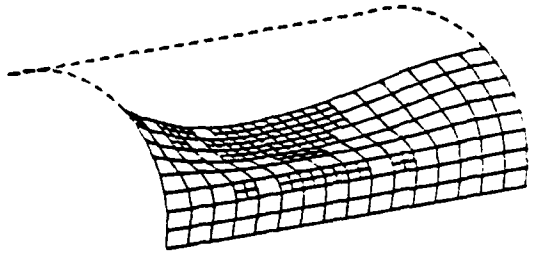

0.300 MS

Figure 16

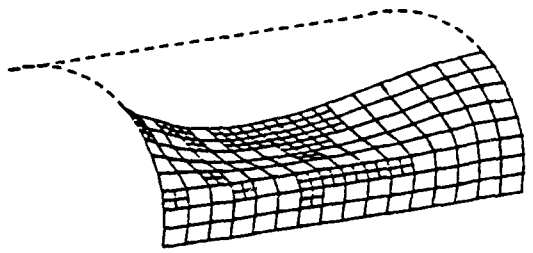

0.350 MS

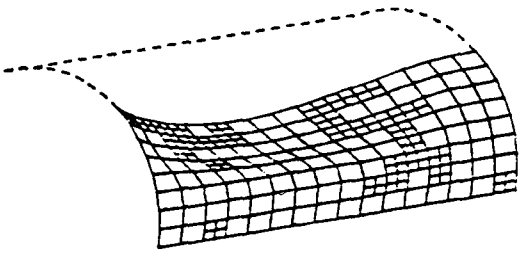

0.700 MS

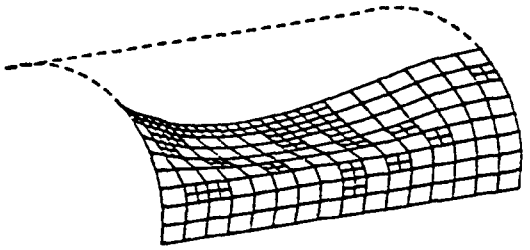

0.400 MS

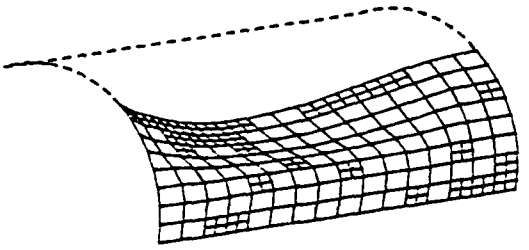

0.800 MS

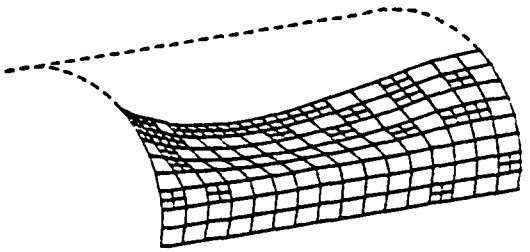

0.500 MS

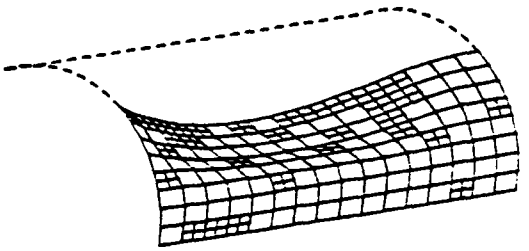

0.900 MS

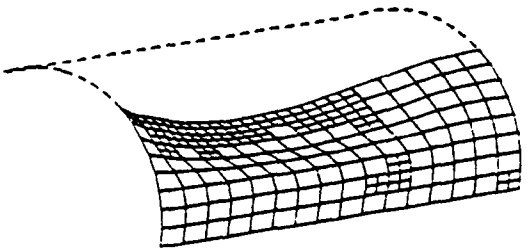

0.600 MS

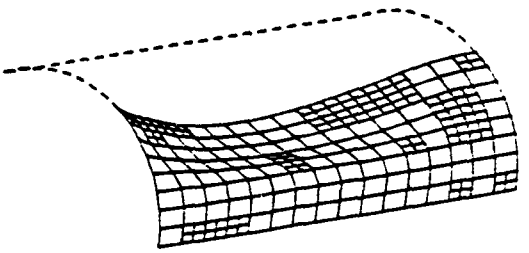

1.000 MS

Figure 16 (Continued)

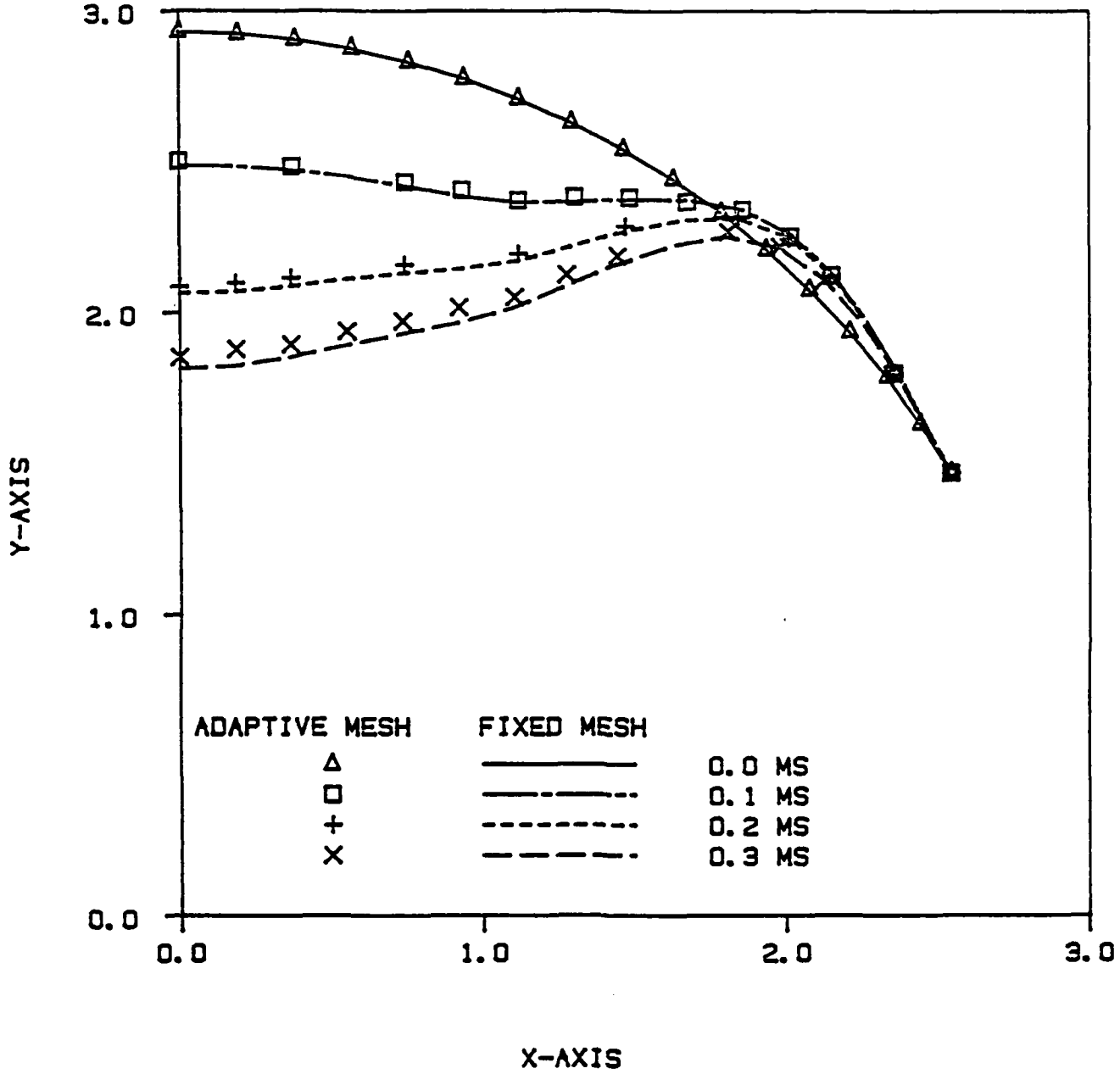
3.0
2.0
1.0
0.0
Y-AXIS
0.0
1.0
2.0
3.0
X-AXIS
ADAPTIVE MESH
FIXED MESH
0.0 MS
0.1 MS
0.2 MS
0.3 MS

Figure 17

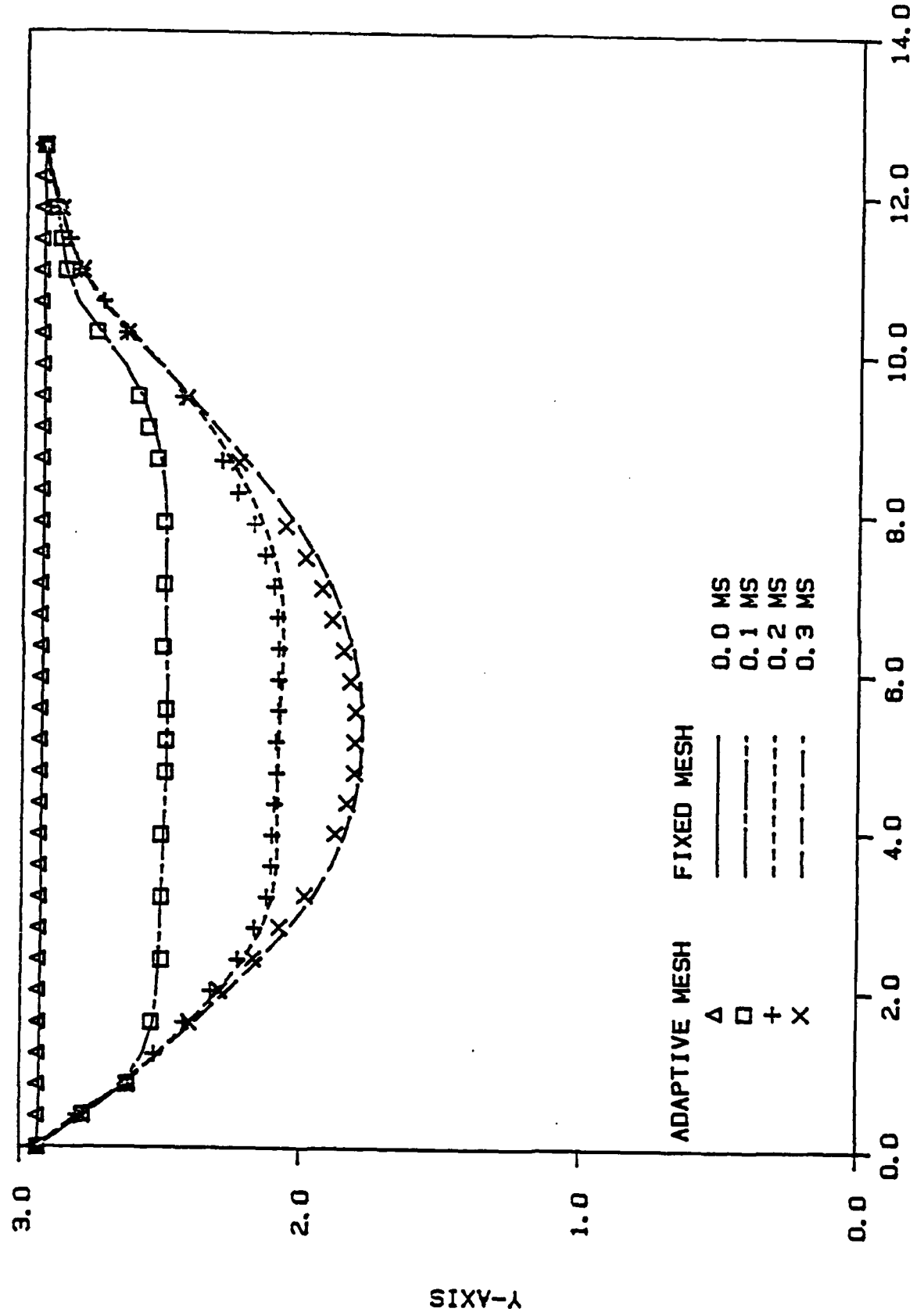
ADAPTIVE MESH
FIXED MESH
Δ
□
+
X
0.0 MS
0.1 MS
0.2 MS
0.3 MS
Y-AXIS
Z-AXIS
0.0
1.0
2.0
3.0
0.0
2.0
4.0
6.0
8.0
10.0
12.0
14.0

Figure 18

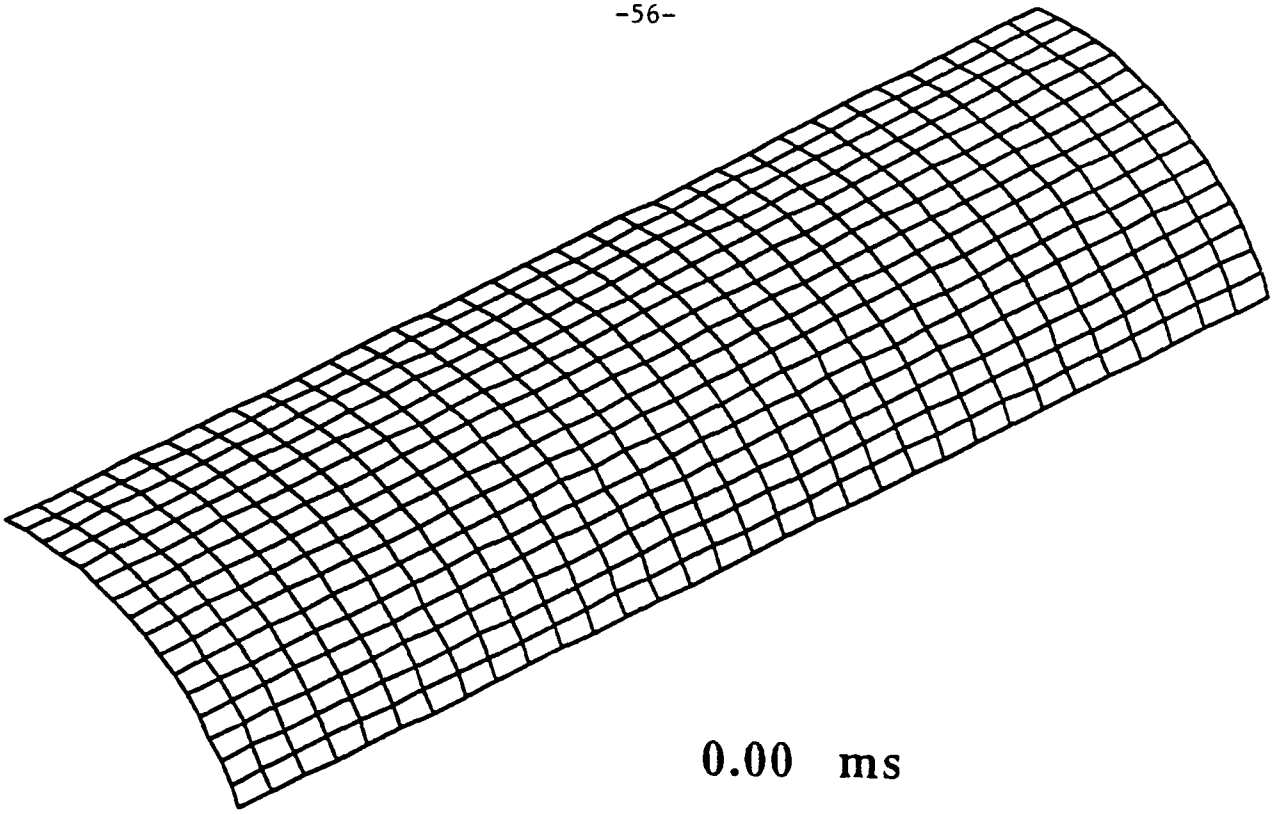

0.00 ms

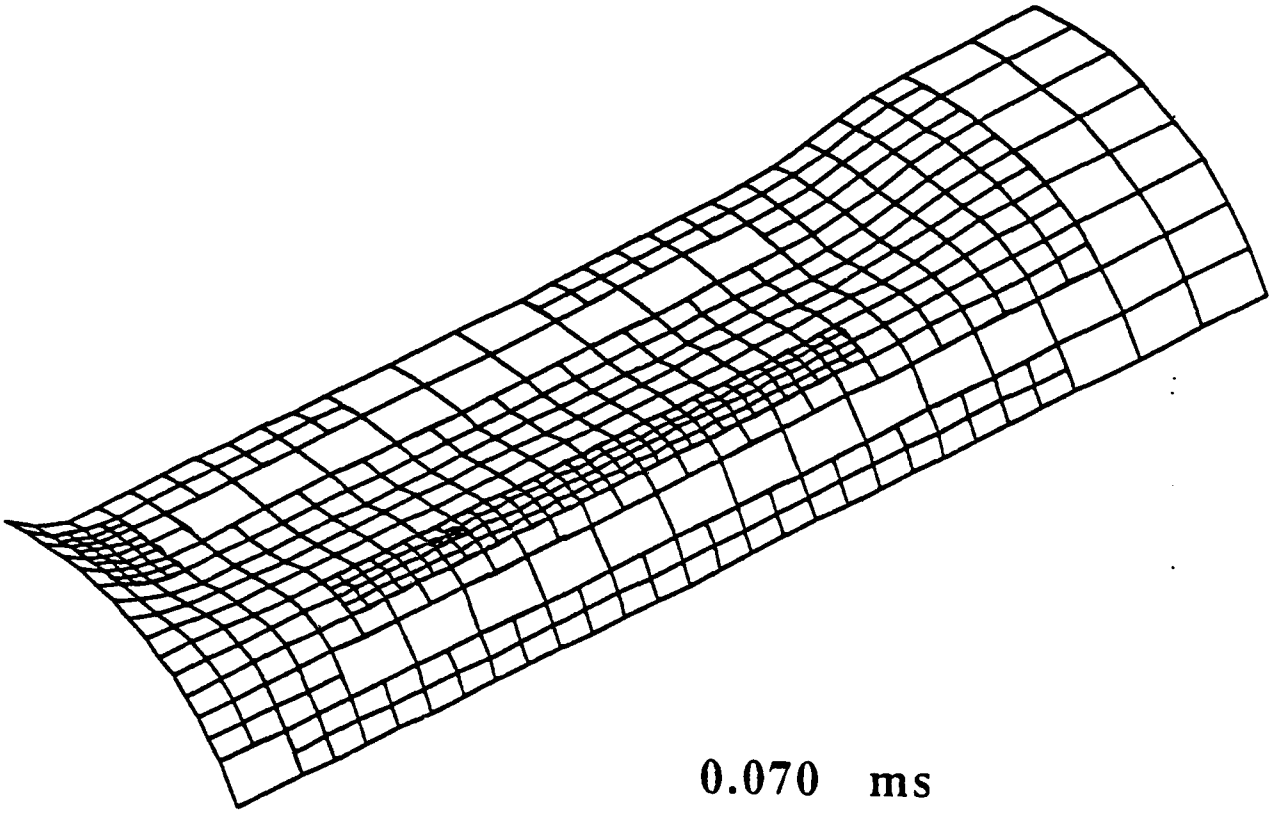

0.070 ms

Figure 19

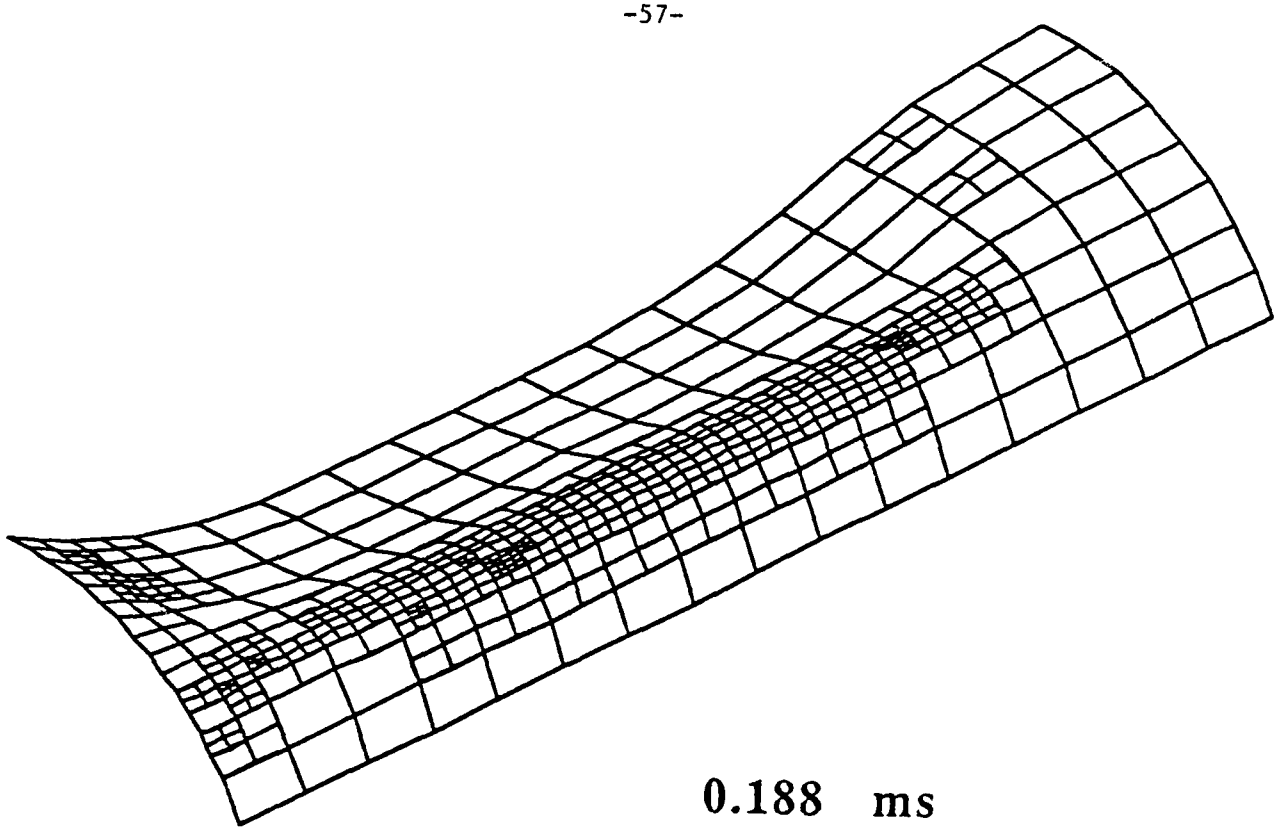

0.188 ms

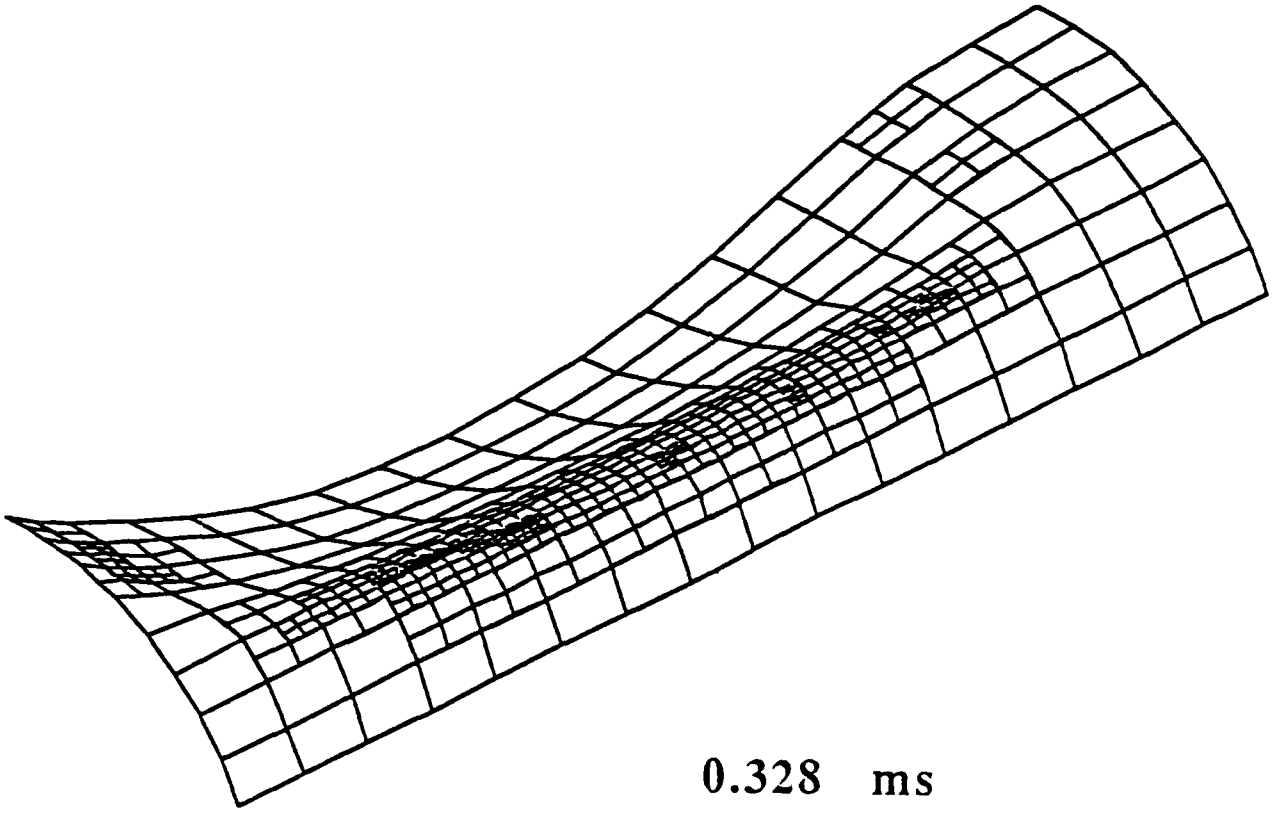

0.328 ms

Figure 19 (Continued)

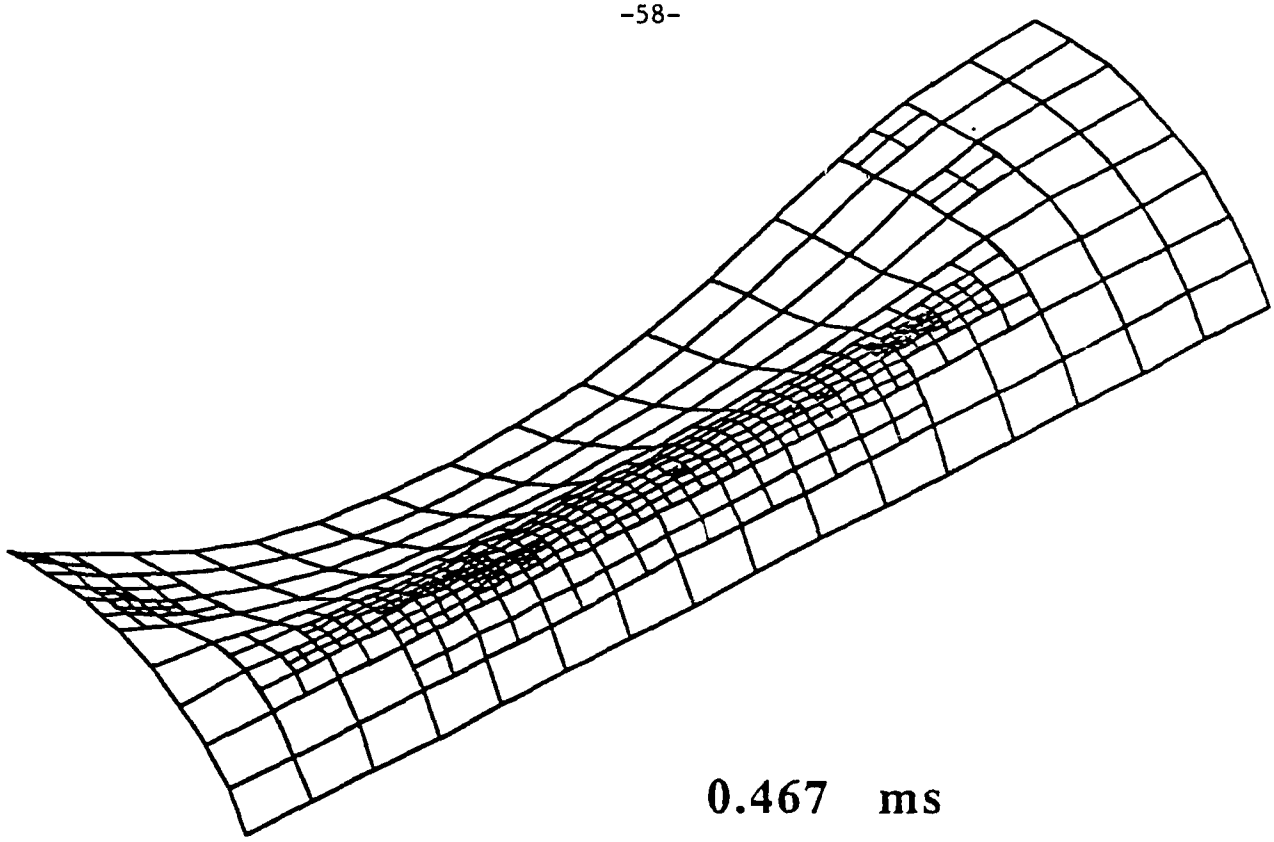

0.467 ms

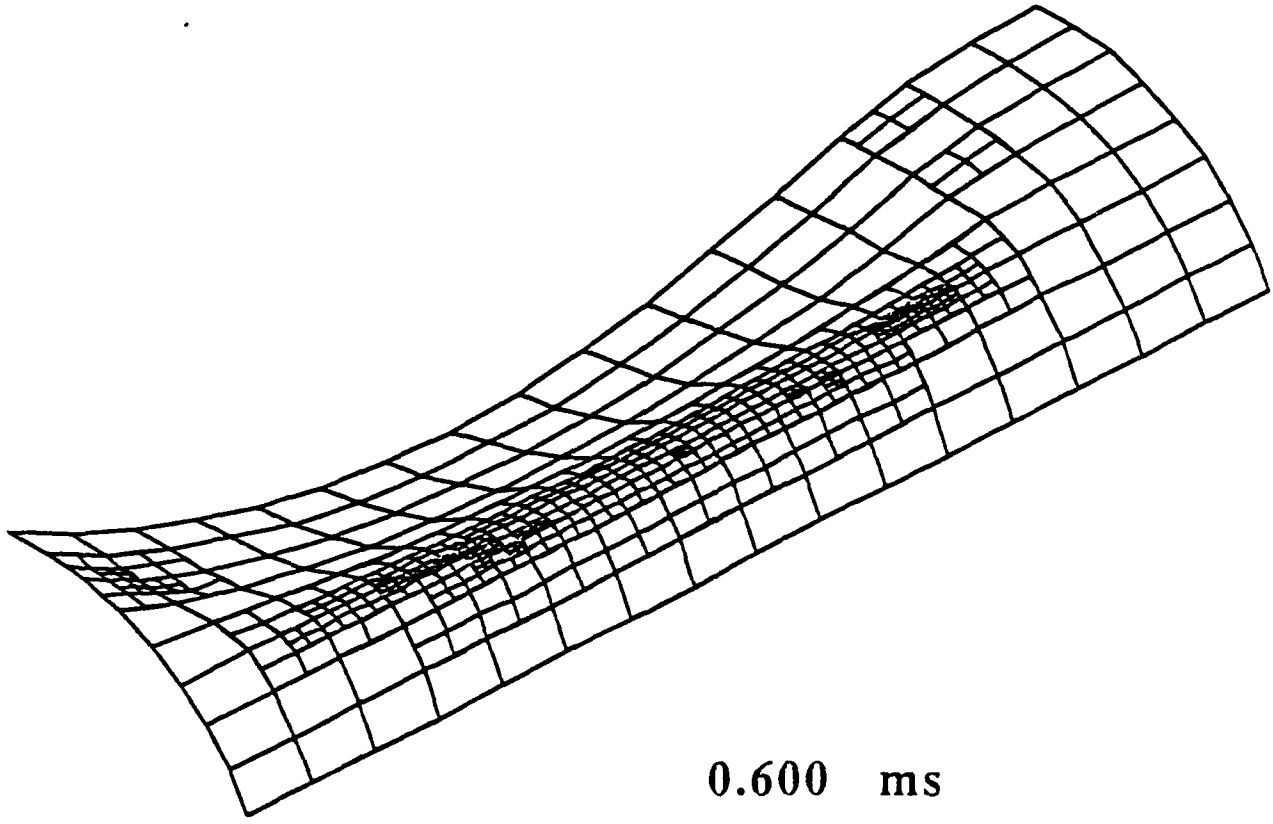

0.600 ms

Figure 19 (Continued)

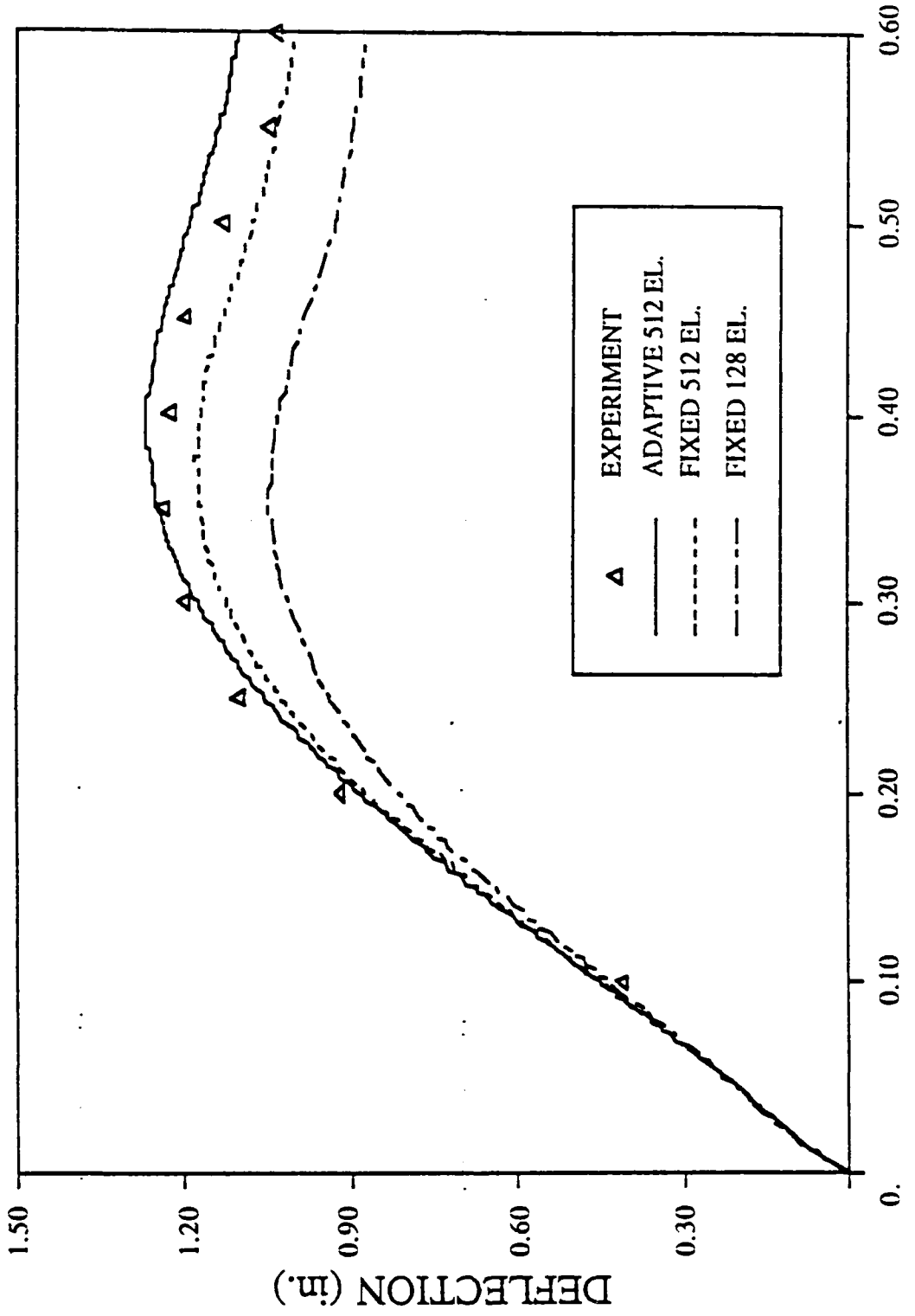
DEFLECTION (in.)
1.50
1.20
0.90
0.60
0.30
0.
0.10
0.20
0.30
0.40
0.50
0.60
TIME (msec.)
EXPERIMENT
ADAPTIVE 512 EL.
FIXED 512 EL.
FIXED 128 EL.

Figure 20

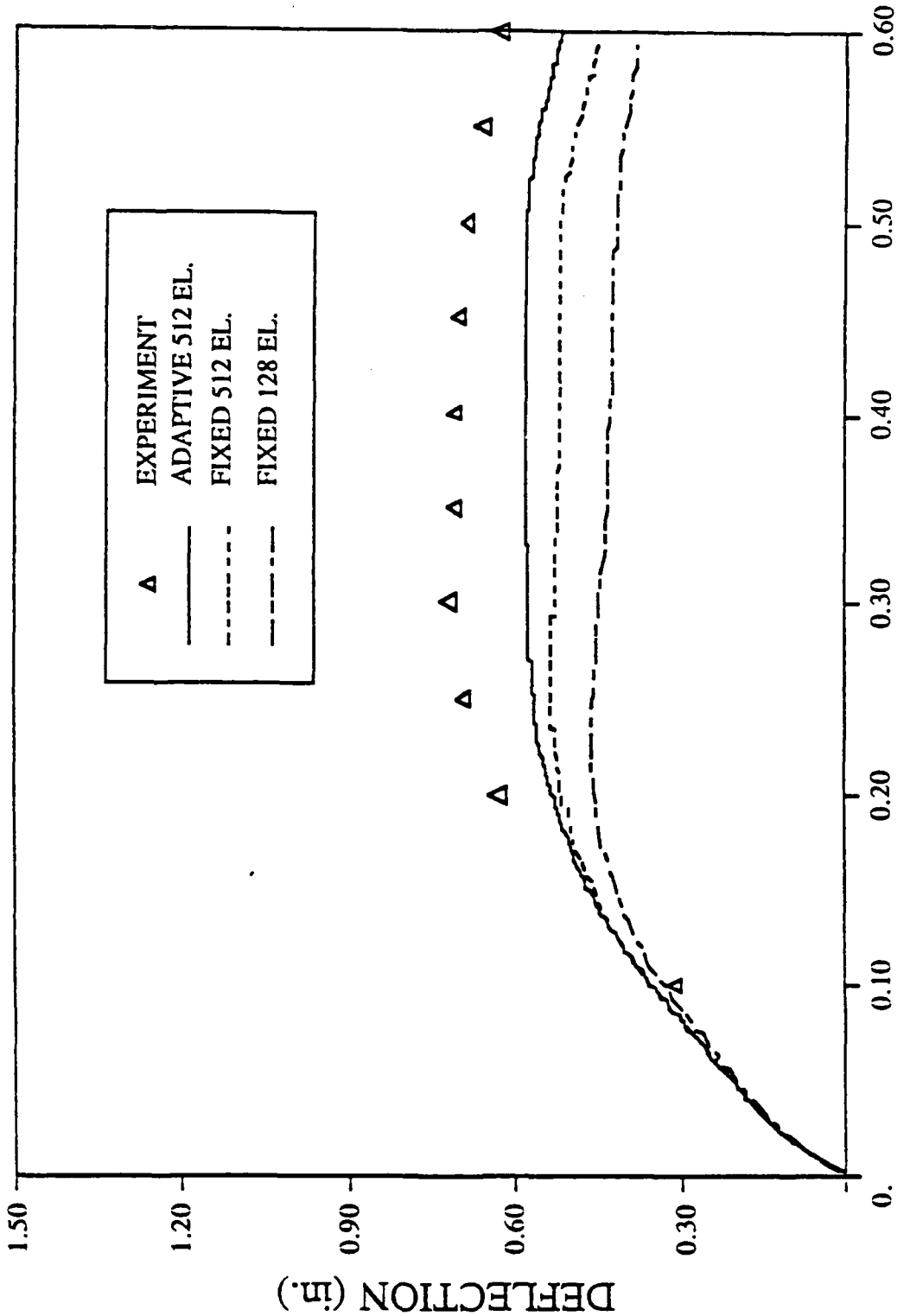
EXPERIMENT
ADAPTIVE 512 EL.
FIXED 512 EL.
FIXED 128 EL.
DEFLECTION (in.)
1.50
1.20
0.90
0.60
0.30
0.
0.10
0.20
0.30
0.40
0.50
0.60
TIME (msec.)

Figure 21

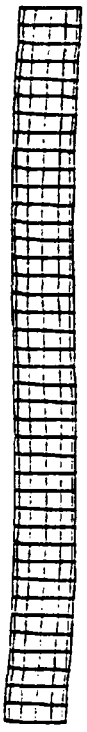

0.0 msec

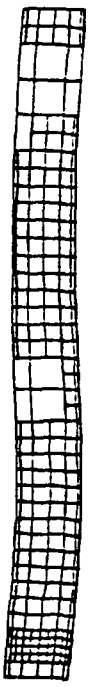

0.17 msec

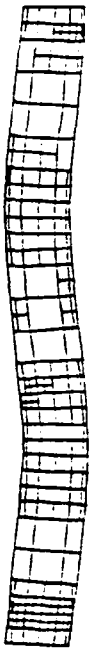

0.30 msec

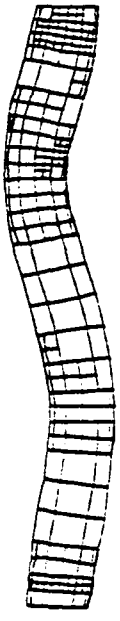

0.47 msec

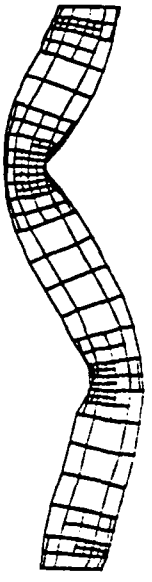

0.64 msec

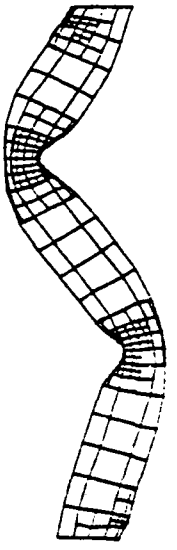

0.80 msec

Figure 22

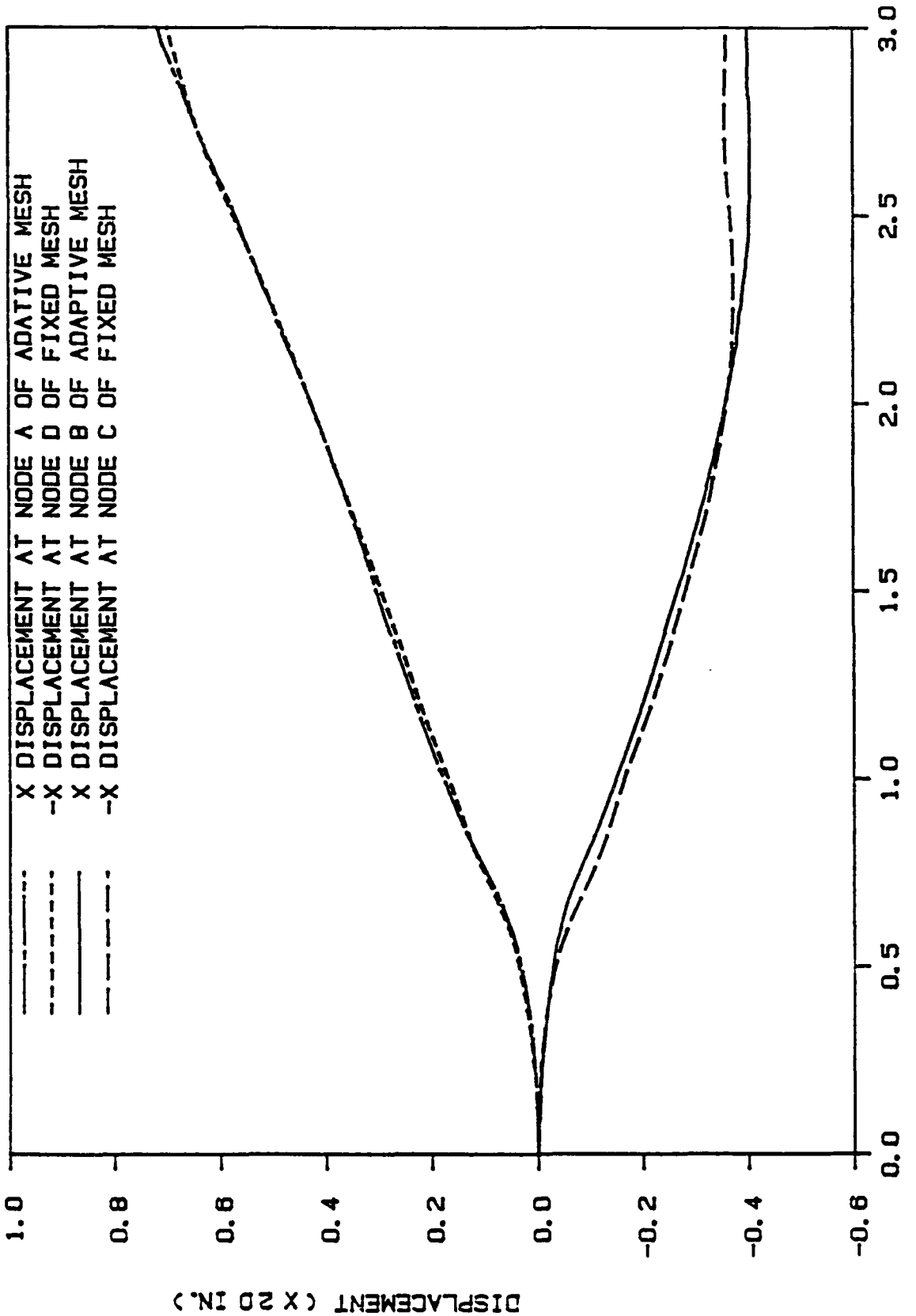
X DISPLACEMENT AT NODE A OF ADATIVE MESH
-X DISPLACEMENT AT NODE D OF FIXED MESH
X DISPLACEMENT AT NODE B OF ADAPTIVE MESH
-X DISPLACEMENT AT NODE C OF FIXED MESH
DISPLACEMENT (X 20 IN.)
TIME (MSEC.)
1.0
0.8
0.6
0.4
0.2
0.0
-0.2
-0.4
-0.6
0.0
0.5
1.0
1.5
2.0
2.5
3.0

Figure 23